

POLITECNICO DI TORINO – HAUTE ÉCOLE D'INGÉNIEURIE  
ET DE GESTION DU CANTON VAUD

Master's Degree in Environmental Engineering,  
course of Climate Change



**Politecnico  
di Torino**

**HE<sup>VD</sup>  
IG**

**HAUTE ÉCOLE  
D'INGÉNIEURIE  
ET DE GESTION  
DU CANTON  
DE VAUD**

Master's Degree Thesis

**Monitoring Bonnard rock glacier under the effect of climate change**

Supervisors:

Prof. Daniele MARTINELLI  
Prof. Erika PRINA HOWALD

Candidate:

Coralie VICARI

October 2024

## Abstract

The purpose of this work is to consider the effects of climate change, specifically of global warming, on an alpine periglacial environment.

The analysis is focused on the mechanical and morphological deformations of Bonnard rock glacier from the data obtained over 11 years, which are mainly from aerial photogrammetry and an in situ global positioning system.

The acceleration of the surface material, namely rocks and boulders, becomes more evident during this time frame, going to increase lava streams and debris flows on Pétérey torrent and to endanger, in such a way, Zinal village, located at the foot of the slope.

## Table of Contents

Abstract .....	2
List of Figures .....	5
Introduction .....	9
The problem of climate change and its action on Alpine environment and glaciers .....	9
Focus on rock glaciers.....	9
1. Chapter 1 .....	14
1.1 Site description.....	14
Problem definition.....	17
2. Chapter 2 .....	19
2.1 Aim of the work .....	19
2.2 Adopted methodology .....	19
3. Chapter 3: Qualitative analysis .....	21
3.1 Aerial photogrammetry .....	21
4. Chapter 4: Quantitative analysis .....	27
4.1 Meteorological data.....	27
4.2 GPS system preview.....	43
4.3 Slope analysis.....	44
4.4 GPS system analysis.....	52
4.5 Fixed GPS .....	57
4.6 Velocity's analysis .....	66
4.6.1 General velocity's maps overview .....	66
4.6.2 Years from 2007 to 2017.....	70
4.6.3 Period from 2010 to 2016.....	72
4.6.4 Short period: two years .....	73
5. Chapter 5: Final comparison .....	75
6. Chapter 6: Mitigation and adaptation strategies.....	79
Conclusions .....	81



## List of Figures

Figure 1 : Schema of a longitudinal cross-section of the internal structure of an active rock glacier (M. Rogora, 2020).....	11
Figure 2 : Schematic classification of rock glaciers with cause-effect relation.....	13
Figure 3 : Location of Bonnard rock glacier.....	14
Figure 4 : Principal features of the slope behind Zinal, from (M. Stoffel, 2009).....	14
Figure 5 : Geomorphological map of Bonnard rock glacier.....	15
Figure 6 : How a rock glacier appears: the Bonnard rock glacier.....	15
Figure 7 : a) Debris along Pétérey torrent; b) How lava stream looks like; c) Schema of a lava streams with the principal components; d) Lava streams which destroyed the principal road for the access to Anniviers valley, family photo, @ Jean-Pierre Genoud, period 1950-1959.....	16
Figure 8 : Construction of a « dépotoir », 2003 vs 2007.....	17
Figure 9 : Mitigation works and variations due to lava streams and debris flows through years : a. 2007 ; b.2012 ; c. 2013 ; d. 2016 ; e. 2017 ; f. 2020, from LANDSAT images.....	18
Figure 10 : Work at the retention basin on Pétérey torrent (2017).....	18
Figure 11 : Location of Zinal village with respect to the rock glacier and to Pétérey torrent, from Google Earth.....	19
Figure 12 : Swisstopo's main interface.....	21
Figure 13 : Location of the blocks under analysis in Bonnard glacier, from Swisstopo, 2020	22
Figure 14 : Displacement during the period 2007-2020 of the rocks 1 and 2.....	23
Figure 15 : Displacement during the period 2010-2016 of three rocks.....	23
Figure 16 : Temperature increasing trend from 1864 to 2023.....	24
Figure 17 : Zoom on the blue area through different years: surface's deformations are visible as time passes: a. 2007, b. 2009, c. 2010, d. 2012, e. 2014, f. 2016, g. 2017, h. 2020.....	24
Figure 18: Displacements of the area in analysis (the one considered for the GPS – see Chapter 4.2 ) with respect to 2007: a. 2007 vs 2010; b. 2007 vs 2012; c 2007 vs 2013; d. 2007 vs 2017; e. 2007 vs 2020.....	25
Figure 19 : Movements on the upper part of the glacier with an highlight on the new boulder.....	26
Figure 20 : Deformations in the surface at the origin of the glacier during different years: a. 2007, b. 2010, c. 2012, d. 2014, e. 2017, f. 2020.....	26
Figure 21 : The three station's location with respect to Bonnard rock glacier (blue perimeter).....	27

Figure 22 : Annual precipitation recorded at “Evolène” station .....	28
Figure 23 : Annual precipitation at “Evolène” station without considering 2007 .....	28
Figure 24 : Annual temperatures' trend at “Evolène” station together with a rough estimation at glacier's elevations.....	29
Figure 25 : « Tracuit » station’ s position (yellow point) with respect to Zinal, from IMIS ...	30
Figure 26 : Annual air temperature at Tracuit station and the projection at 2850 m .....	30
Figure 27 : Air temperature variations through years with mean trends calculated for 2007 and 2023 .....	31
Figure 28 : Monthly temperature per year with respect to the mean over the considered period .....	33
Figure 29:Monthly ground, surface snow, air and active layer temperature.....	36
Figure 30 : Temperature trends respectively of ground, active layer, air and snow surface....	37
Figure 31 : Simplified model of hydrological functioning of a rock glacier, with possible precipitation paths .....	38
Figure 32 : Precipitation typology at “Evolène” station between 2007 and 2023 .....	39
Figure 33 : Annual snowfall recorded at “Evolène” station.....	39
Figure 34 : Precipitation typology at “Tracuit” station .....	40
Figure 35 : Annual snowfall recorded at “Tracuit” station .....	40
Figure 36 : Annual snowpack height.....	41
Figure 37 : Trends of annual snowfall and snowpack.....	42
Figure 38 : Bedrock’s roof, visualization in SAGA software and its location with respect to the hill, displayed in QGIS software .....	44
Figure 39 : The plan curvature A. convex surface, B. concave surface.....	44
Figure 40 : The profile curvature : A. convex surface, B. concave surface .....	45
Figure 41 : Slope of bedrock’s roof, 2D visualization in SAGA .....	45
Figure 42 : 3D view of slope parameter .....	45
Figure 43 : Aspect of bedrock’s roof, 2D visualization in SAGA .....	46
Figure 44 : Profile and Plan curvature of bedrock’s roof, 2D visualization in SAGA .....	46
Figure 45 a. 2D view of the bedrock’s roof on the numerical model (DEM), b. 3D view, in SAGA.....	47
Figure 46 : DEM’s slope .....	47
Figure 47 : DEM’s aspect.....	48
Figure 48 : DEM’s profile and plan curvature .....	48
Figure 49: Elevation difference in 2D and in 3D visualization.....	49

Figure 50 : Elevation difference in 2D and in 3D visualization.....	49
Figure 51 : Slope difference in 2D and in 3D visualization.....	50
Figure 52 : Aspect difference .....	50
Figure 53 : Profile and plan curvature differences .....	51
Figure 54 : GPS points in the area.....	52
Figure 55 : Example of GPS points' motion from 2007 to 2018 .....	52
Figure 56 : Manual length measurement in QGIS .....	53
Figure 57 : Length of all displacements of rock glacier's surface material .....	54
Figure 58 : Flow direction map with arrows .....	54
Figure 59 : Focus to see complete series of 80 points on the area of interest .....	55
Figure 60 : 80 points mean elevation .....	55
Figure 61 : Depth of material in motion with the relative variation in depth from one year to another.....	56
Figure 62 : Fixed GPS 's location with respect to the whole glacier and to the bedrock's roof .....	57
Figure 63 : Elevation of fixed GPS .....	57
Figure 64 : Fixed GPS with respect to the slope of the bedrock's roof .....	58
Figure 65 : Fixed GPS with respect the aspect of the bedrock's roof.....	58
Figure 66 : Annual displacement of fixed GPS.....	59
Figure 67 : Environmental data at "Tracuit" station from 2010 and 2023.....	60
Figure 68 : Mean winter air temperature and typology of recorded precipitation .....	61
Figure 69 : Mean winter precipitation and snowpack at "Tracuit" station .....	61
Figure 70 : Mean winter displacement of GPS1 .....	62
Figure 71 : Mean winter displacement of GPS2 .....	63
Figure 72 : Mean summer air temperature and typology of recorded precipitation .....	63
Figure 73 : Mean winter precipitation and snowpack at Tracuit station .....	64
Figure 74 : Mean summer displacement of GPS1.....	64
Figure 75 : Mean summer displacement of GPS2.....	65
Figure 76 : Mean displacements in winter and in summer .....	65
Figure 77 : Mean velocity of the area coinciding to the bedrock's roof .....	66
Figure 78 : Speed map 2007-2008 .....	67
Figure 79 : Speed map 2008-2009 .....	68
Figure 80 : Speed map 2009-2010 .....	68
Figure 81 : Speed map 2010-2011 .....	68

Figure 82 : Speed map 2011-2012 .....	69
Figure 83 : Speed map 2012-2015 .....	69
Figure 84 : Speed map 2015-2016 .....	69
Figure 85 Speed map 2016-2017 .....	70
Figure 86 : Speed difference map calculated between 2007 and 2017 .....	70
Figure 87 : Zoom on fixed GPS with respect to speed intensity variation between 2007 and 2017.....	71
Figure 88 : Zoom on fixed GPS with respect to speed intensity variation between 2010 and 2016.....	73
Figure 89 : Speed difference map calculated between 2007 and 2009 .....	73
Figure 90 : Speed difference map calculated between 2015 and 2017 .....	74
Figure 91 : Orthophotos of 2009 (left) and 2010 (right) with the moving areas.....	75
Figure 92 : Speed map 2009-2010 on the corresponding ortophoto .....	75
Figure 93 : Ortophotos of 2016 (left) and 2017 (right) .....	76
Figure 94 : Speed map 2016-201 7 on the corresponding ortophoto .....	76
Figure 95 : Area measurement with QGIS around SPOT1 .....	77
Figure 96 : Area measurement with QGIS of lobe 1.....	77
Figure 97 : TLS from <a href="https://geosurveyengineering.co.ke/terrestrial-laser-scanning/">https://geosurveyengineering.co.ke/terrestrial-laser-scanning/</a> .....	79
Figure 98 : Photograph from a borehole camera from (L. Arenson, Borehole deformation measurements and internal structure of some rock glaciers in Switzerland, 2002) on the left; borehole implementation from (J. Noetzli L. A., 2021) on the right .....	80



## Introduction

The problem of climate change and its action on Alpine environment and glaciers

Greenhouse gases emissions deriving from human activities are the main cause of global warming in the last decades: the mean increment of temperature is around + 1.1°C, higher over lands than over oceans. This induced change is already affecting weather and climate all around the World (IPCC, 2023).

In this context, both high-mountain alpine glacial and periglacial environments are considered as a wake-up call because of their huge sensitivity to thermal changes (UNEP, 2008): over the 20th century, the air temperature increment on mountainous areas has been twice than that on a planetary scale, meaning that an amplification of the phenomenon exists (M. Chiarle, 2008).

Direct consequences are a general lower elevation in snow cover together with mass movements of ice and rocks which are increasing year by year, affecting overall the stability of bedrock, debris slopes and glaciers with visible effects, even from naked eye. More difficult to be detected are the effects on permafrost, defined as ground with a temperature lower or equal to 0°C during at least two consecutive years, and its dynamics: only recently, monitoring of such phenomena started, especially in densely populated mountain areas which are more and more exposed to higher levels of hazards with the objective of early warning and prevention.

In the specific, this work is focused on the understanding of the impacts of climate change on permafrost and rock glaciers, which form the so-called periglacial environment. To do so, the case of the Bonnard rock glacier is analysed (I. Gärtner-Roer, 2022).

### Focus on rock glaciers

Considering the cryosphere compartment, the centre of attention of this work are rock glaciers, morphological indicators for permafrost occurrence in high mountain environments (M. Rogora, 2020).

They do not look like conventional glaciers because they have little ice visible at their surface: in fact, they are a mixture of rock, ice, snow, mud and water, in particular defined "mass of ice covered by rock debris or mass of rock with interstitial ice" (Kaufmann, 2012).

All this material, with a general thickness higher than 10 m (R. Delaloye T. S., 2010) flows down (with higher or lower speed, variable on a timescale of days, season or decades) due to the gravity force's effect giving the typical elongated and lobate shape with over-steepened fronts and lateral talus; series of ridges and furrows on the surface are a hallmark, reflecting the internal process of deformation, which occurs at the so-called "shear horizon" level (J. Noetzli C. P., 2023) making them to look like lava flows.

General and common characteristics for all the rock glaciers can be summarized as follows ((SSGm), 2020):

- a chaotic aspect with wrinkles and furrows on the surface;
- a deep and unstable front;
- a sorting of materials with coarse elements remaining on the surface (thus, anisotropic material properties);
- the presence of interstitial ice or buried massive ice;
- a slow creep movement from a few centimetres to several meters per season and/or year.

For this last attribute, in reference to their kinematics, they are called "active rock glaciers" or "sediment cascades", to distinguish them from the "inactive" ones, which instead don't move downslope and have few or no internal ice.

Moreover, they generally present three distinguished layers (R. Delaloye T. S., 2010) (A. Cicoira, 2020; M. Rogora, 2020): the shallow one (also called "active layer" which freezes and thaws seasonally) and the lowermost are made of large boulders, while in the middle there is an ice-rich permafrost layer with a mixture of ice and debris.

The active layer is the interface with the atmosphere and it is mainly composed of rock, ice, water and air fraction (multiphase nature); it influences the rock glacier dynamics for its role played on the mass and the energy balance. Its thickness depends on meteorological characteristics, accumulation and duration of snow cover and the textural characteristics of the active layer itself (W. Haeberli B. H., 2006).

The ice-rich core has a general thickness of 10-25 m and it is composed of debris which grain size is finer than in the upper layer.

Finally, the shear horizon, at a depth of 15-30 m, shows high shear rates and moreover the majority of deformations occur here.

The ablation zone is in particular completely covered by debris, while the accumulation one coincides with the avalanche cone; the ELA (Equilibrium Line Altitude), which is the area where the accumulation is balanced by the ablation over a one year period, is above the land surface, meaning that the rate of local melt is higher than the rate of local snowfall (R.S. Anderson, 2018).

The major parameter of destabilization of a rock glacier is surely the topography of the ground surface: in fact, a very steep slope implies a high shear stress near the base of the system and secondly, the typical convex bedrock which, as mentioned, creates a flow pattern, contributes to rock glacier's thinning (R. Delaloye S. M., Rapidly moving rock glaciers in Mattertal, 2013).

In addition, basically, also the plastic deformation of internal ice is another important cause of destabilization.

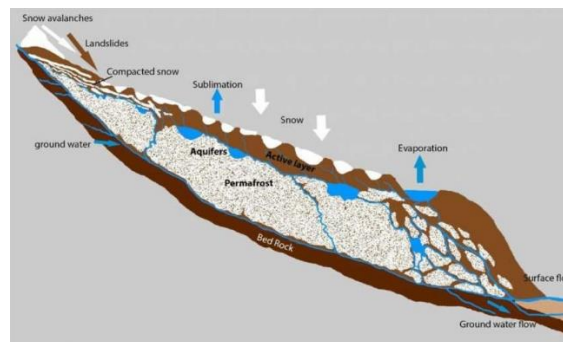


Figure 1 : Schema of a longitudinal cross-section of the internal structure of an active rock glacier (M. Rogora, 2020)

During the last decades, climate change began to have important consequences on the periglacial environment: it is important to underline that (W. Haeberli B. H., 2006) the depth of the shear horizon affects the influence of surface temperature on it: its forcing results to be limited and especially delayed in time. But at longer time scales, variations in temperature, as it is recently occurring, are able to affect the mechanical properties of the rock glacier at the depth of the shear horizon!

From data, it appears that a relation can be established between atmospheric warming, extreme heat waves and the acceleration and destabilization of rock glaciers, together with an evident thinning in the accumulation zone and an increment in the melting rate below debris (P. Deline, 2015; R. Delaloye S. M., Rapidly moving rock glaciers in Mattertal, 2013).

This brings to several repercussions namely a lower ice viscosity closer to the melting point, the onset of basal sliding and an increment of unfrozen pore water, all factors which contribute to enlarge slope instability, especially rock glacier acceleration, rock falls, landslides, debris and water flows, impacting vegetation coverage and runoff patterns. Temperature increment influences both the rheological properties of ice and the flow/permafrost creep velocity of rock glaciers, which are for this reason considered as an indicator of the environmental changes in cold mountains.

In fact, the rapid increment of air temperature in European Alps, observed since 1980s, has warmed the permafrost of about 0.5-1°C with, as result, an acceleration of the rock glaciers creep especially during 1990s and 2000s (P. Deline, 2015; R. Delaloye T. S., 2010).

Overall, rock glacier's geometry evolution, deformation rate and consequent slope instability are strictly related both to internal and external causes.

As previously mentioned, the internal factors are of geometrical, topographical, mechanical nature, while the external ones are especially thermal, hydrological and glaciological or related

to possible overloading of rock glacier triggered by landslides or rock falls (R. Delaloye S. M., Rapidly moving rock glaciers in Mattertal, 2013; (SSGm), 2020).

A strong relationship exists between these factors: with an increment of rock temperature, water percolation implicates a loss of joints bonding and a reduction in hydraulic permeability and mechanical strength which alters the stress field, decreasing the safety factor of the slope and causing consequently destabilization, dislocation, debris flows and even collapse (P. Deline, 2015; M. Davies, 2001). In fact, temperature variations, and so the transition from the frozen to the thaw state, have important effects on the related cohesion and friction angle of the soil (E. P. Howald, 2023).

Especially during the melting season or heavy rainfall events, rock glacier's advance increases and it can be summarized into four main processes: cohesion loss of sediments due to the thaw in the matrix, cohesion reduction due to creeping, spatio-temporal changes in water circulation and constant rejuvenation of sediments on the slope. (E. Bardou G. F.-B.-D., 2011).

From a kinematics point of view, (A. Kääh T. R., 2005) generally, an accepted conceptual model for rock glacier advance, is the so-called "conveyor belt effect": the material from the upper layers overrides the lower ones, then it is deposited in the front of the glacier and it is finally overridden by new material from upper layers. This mechanism depends on four key aspects:

- vertical variation of the horizontal velocity;
- volume;
- air content;
- erosion and removal of solid material.

Clearly all these characteristics differ from one glacier to another and for that reason a classification of these geomorphological landforms exists, with a subdivision in five typologies, depending on the speed of the deformation (P. Deline, 2015):

- Type I: moderate multi-annual velocity fluctuations in the range of a centimeters per year to  $> 2\text{m/year}$ ;
- Type IIa: accelerated displacement of a rock glacier with opening of crevasses or scarps on the surface;
- Type IIb: very strong acceleration with speed up to  $> 80\text{ m/year}$ ;
- Type III: acceleration and dislocation of the lower part of a rock glacier, with the formation of scarps;

- Type IV: collapse of the lower part of the rock glacier, which breaks down as a debris flow; a new front develops from the scarp.

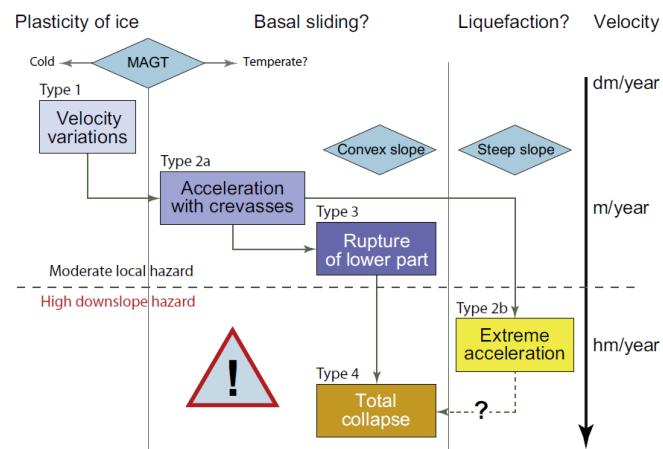


Figure 2 : Schematic classification of rock glaciers with cause-effect relation

From here on out, the focus will be on the Bonnard rock glacier, which is part of the third typology, as it will be discussed in the following section.

# 1. Chapter 1

## 1.1 Site description

The study area is the Glacier Bonnard located in the Val d'Anniviers, Valais, Switzerland, overlooking the Zinal village (46° 8.057' N and 7° 39.411' E). It is approximately long 1000 m, 150-300 m wide and with an average thickness of 15-20 m.

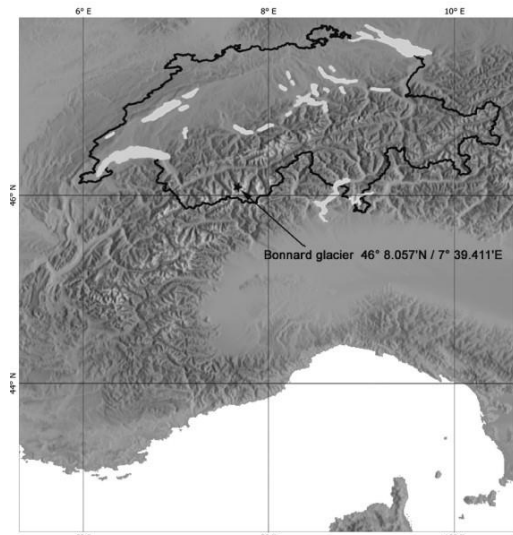


Figure 3 : Location of Bonnard rock glacier

The altitude ranges from 2800 to 3100 m (M. Rogora, 2020), below the Diablons summit (3609 m): the rock glacier is in the middle between two moraines and it lies on a moraine bastion, composed at 60% of creeping permafrost which supplies loose material, from which two torrents originate: Tracuit and Pétérey (E. Bardou G. F.-B.-D., 2011). The considered area is about 3 km<sup>2</sup>, of which the source area represents 1.7 km<sup>2</sup>.

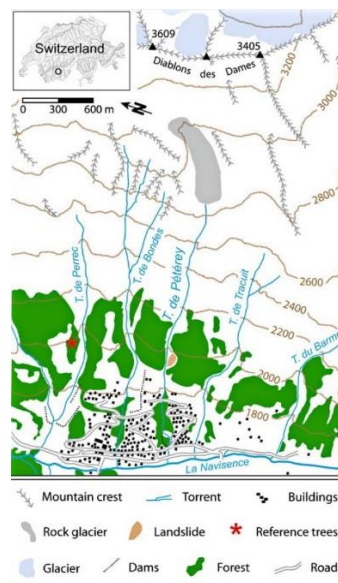


Figure 4 : Principal features of the slope behind Zinal, from (M. Stoffel, 2009)

From a geological point of view, the Bonnard glacier is made of rock debris of granitic gneisses and crystalline schists coming from the cliffs of the Diablons (E. Bardou G. F.-B.-D., 2011; E. P. Howald, 2023; M. Rogora, 2020). The outcrops around both glacier and moraine are made of gabbros; scree fans surround the glacier system and, below the source area, hanging till are present.

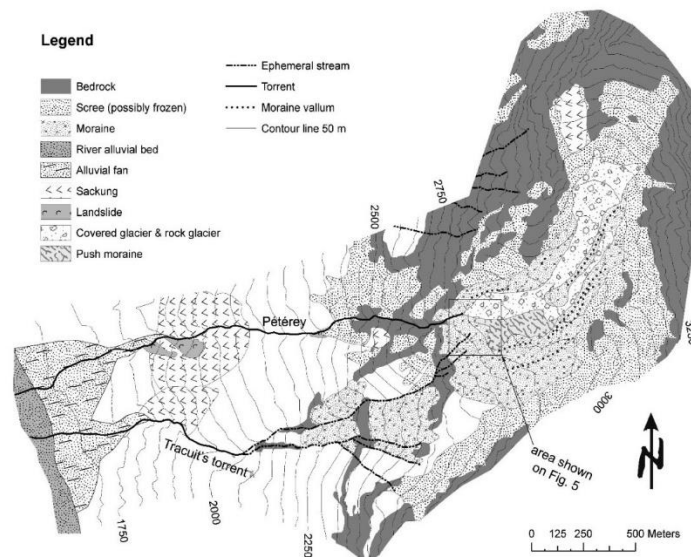


Figure 5 : Geomorphological map of Bonnard rock glacier

Moreover, the slope is quite steep ranging between 40 % to more than 80 %, with an evident shelf break between the upper and the lower part.



Figure 6 : How a rock glacier appears: the Bonnard rock glacier

From summer to autumn, heavy rainfall events, strong glacier melting, but also warm periods without rainfall, related to the atmospheric warming, are the main causes of lava streams, consisting of water, mud and rubbles, in that area: the geologist Guillaume Favre-Bulle, who works for CREALP (Centre de recherche sur l'environnement alpin) in Sion, studying the

phenomenon affirm that "c'est un système très dynamique parce que la glace s'est réchauffée et qu'elle fond jusqu'à 2,5 mètres de profondeur en été" (Le Temps, 2017).

As a result, water mainly feeds the northern part of the moraine, producing a mean of one to three of these events per year in the Pétérey torrent, where therefore the sedimentary activity results to be very important.

These phenomena are very powerful and destructive and they have been recorded through years. For a total of 15 major events, the more relevant, which appears in literature, are the ones of 1929, 1936, 1950, 1956, 1970, 1987, 2008 and 2012 (G. Bertoldi, 2012). In fact, already in 1948, the scientist Ignace Mariétan wrote: "Tout ce versant est en pleine désagrégation; de tout temps l'activité de ces torrents a été très intense; elle se manifeste surtout par des coulées de pierres".

Instead, in Tracuit torrent, debris flow are less frequent and only two main events are reported (the biggest is the one of 1987).

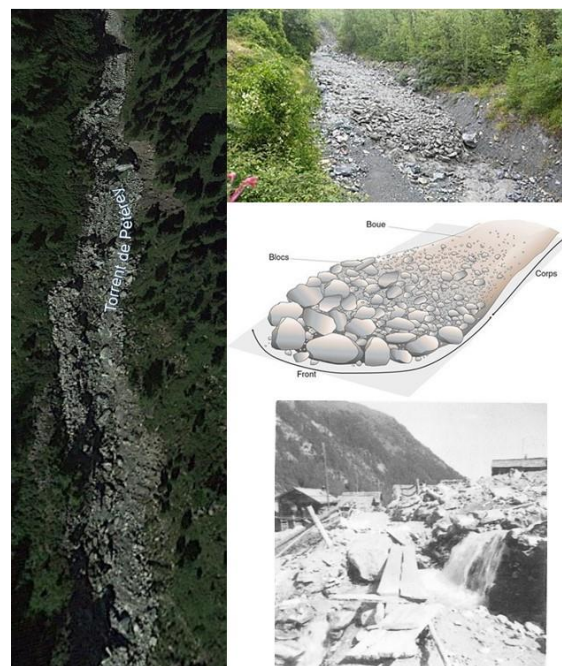


Figure 7 : a) Debris along Pétérey torrent; b) How lava stream looks like; c) Schema of a lava streams with the principal components; d) Lava streams which destroyed the principal road for the access to Anniviers valley, family photo, @ Jean-Pierre Genoud, period 1950-1959



## Problem definition

The monitoring of glacier's activity is fundamental not only for a better understanding of the relationship between climate change, permafrost melting and debris flow, but also because, for a more practical point of view, Zinal village, at 1670 m, is just downstream the Pétérey torrent and so it is endangered by such events.

Some researches conducted directly on the field reveal that the total volume of materials which can be mobilised by lava streams is approximately of 40000 m<sup>3</sup> for Pétérey and 6000 m<sup>3</sup> for Tracuit torrent (B. Einhorn, 2011). In this context, mitigation measures have been adopted to protect the buildings and the ski lift facilities: at present, retention basins, dated 1958, have been enlarged in 2019 to be able to contain more significant lava streams which are expected to increase due to the atmospheric warming. This is a complex system of walls and deflectors called "dépotoirs", which need to be maintained and cleaned, generally in autumn (Parvex, 2013; G. Bertoldi, 2012).

In *Figure 8*, the construction of such structure can be appreciated and the difference is between the years 2003 and 2007:



*Figure 8 : Construction of a « dépotoir », 2003 vs 2007*

Mitigation works are well visible in some aerial images taken from Swisstopo, relating to the years 2007, 2012, 2013, 2016, 2017 and 2020. Some variations of the zones of accumulation of the debris and of the vegetation cover, also related to some lava streams, are detectable until 2016, whereas in 2017 some important works began and the results can be seen 2020 with an imposing retention basin, downstream of Pétérey torrent.



*Figure 9 : Mitigation works and variations due to lava streams and debris flows through years : a. 2007 ; b.2012 ; c. 2013 ; d. 2016 ; e. 2017 ; f. 2020, from LANDSAT images*



*Figure 10 : Work at the retention basin on Pétérey torrent (2017)*

## 2. Chapter 2

### 2.1 Aim of the work

For this work on the Bonnard rock glacier, the purpose is twofold: on one side, it is oriented towards the study of the evolution of its deformations and accelerations during the last decade, in relation with the atmospheric warming; on the other, towards the detection of the most dangerous areas, which can be the main causes of collapses, lava streams and debris flows especially through Pétérey torrent which has already happened, puts at risk Zinal village, at the bottom of the valley.

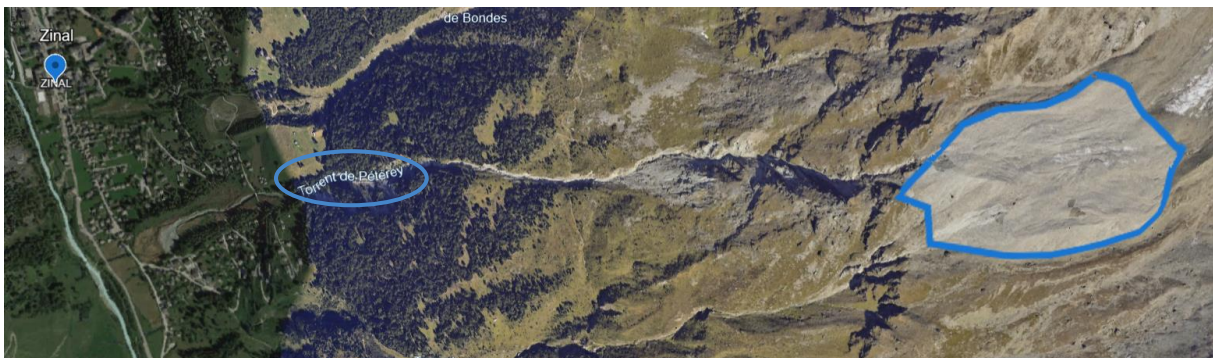


*Figure 11 : Location of Zinal village with respect to the rock glacier and to Pétérey torrent, from Google Earth*

The analysis of the glacier is based on the use of different tools and instruments, both from geophysics and geomatics.

### 2.2 Adopted methodology

Understanding glacier's mechanical behaviour related to temperature raise, as a function of time, in order to be able also to quantify the possible impacts on the environmental field is the fundamental goal of this work, together with the comprehension of where the accumulation zones of debris are situated and can be possible supply areas for lava streams, in order to try to find a relationship between the main deformations and those kinds of events which occur in the torrents.

To do so, a specific methodology is followed, made of four main steps.

First of all, the photogrammetric approach is exploited: the use of georeferenced time-lapse photography (orthophotos) in fact allows an immediate or nearly immediate visual impression of rock slope failures, debris flows or rocks and blocks movements.

By comparing images of different years, in a qualitative way, it is possible to quantify the major displacements of the material at the surface.

Secondly, meteorological-environmental data (namely mean temperature, mean precipitation and mean snowpack height) are analysed both separately, both together to have an overview of the main trends occurring in the area.

Then, GPS system based on different points in situ situated in the lower part of the glacier, together with their relative velocities data, are used in order to detect the movements of the surface, in this case in a quantitative way.

In the specific, the availability of coordinates X, Y and Z for the, more or less, hundreds of GPS points, their velocities' pattern and the total displacements over time of two fixed GPS allow to reach the aim of the study.

In such a way, a relation between raising temperatures, decreasing of glacier's depth, increasing in velocities is established from 2007 to 2018, the period of the monitoring. Furthermore, also the detection of the most unstable areas is conducted.

Finally, a comparison is performed between the results of the first, the second and the third parts in order to understand if they are in agree: the areas which moves at major rates are the same detected also with the photogrammetric data? Are they the main source of debris flows and lava streams?

The answers to these questions allow, to conclude, to find some mitigation and adaptation strategies which should be enhanced or implemented.

### 3. Chapter 3: Qualitative analysis

#### 3.1 Aerial photogrammetry

In order to acquire data related to the movement of Bonnard rock glacier and to document in the meantime the three-dimensional surface kinematics of the creeping mountain permafrost, aerial photogrammetry is used (R. Kenner, 2017). It is considered as the best established remote sensing technology for rock glacier monitoring, allowing to measure both surface displacements both thickness changes (A. Kääh V. K., 2003).

In particular, the changes in surface elevation are mainly related to three fundamental aspects, all visible through the visualization of the orthophotos:

- sediment accumulation or evacuation;
- extension or compression;
- subsidence of the terrain due to thawing of supersaturated permafrost or frost heave because of freezing of water.

The images, namely aerial photographs, are views of landscape photographed from aircraft, freed of their distortions; they are obtained from Swisstopo, the Switzerland Federal Office of Topography and geoinformation centre.

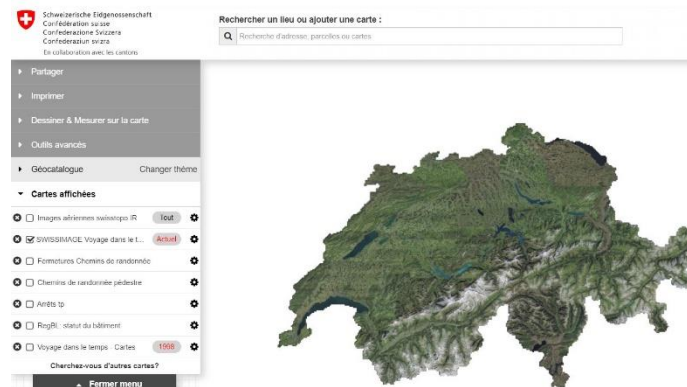


Figure 12 : Swisstopo's main interface

In the specific, in the area of interest, images are available from 1977 and until 1997, they are in black and white and manual corrections concern only clouds removal, with no intervention on distorted objects, dusts and scratches. Whereas, from 1999, colours appear, together with an optimization of image corrections and a consequent increment of the level of accuracy overall: the ground resolution is of 50 cm over the Alps.

Starting from 2005, images are taken using a digital camera, with an improving of ground resolution up to 25 cm.

The adopted coordinate system is LV03 until 2008, while from that year onwards is LV95, the Switzerland's official coordinates with the point of origin located in Bern.

Finally, from 2017, ADS100 digital camera's introduction implicated an enhancement of both ground resolution and planimetric accuracy, which is of  $\pm 1$  m.

The oldest photos are updated every three years, whereas in general the more recent every one or two years: for that reason, they are subdivided into "classes", in order to be able to analyse and to detect the most relevant modifications of the ground.

In particular, these "classes" are:

1977-1979; 1983-1985; 1988-1991; 1992-1994; 1995-1998; 1999-2004; 2005-2006; 2007-2008; 2009; 2010-2011; 2012; 2013; 2014-2015; 2016; 2017-2019; 2020-2024.

For a better and clear appreciation of the dynamic behaviour of the glacier, for this first qualitative kind of analysis, more recent photographs are considered (the ones from 2007) because, as previously mentioned, the resolution is higher.

By overlapping the orthoimages of different years, it is immediately easy to see the movement and the deformation of the surface of the glacier; some rocks located in the lower part of the periglacial complex at the origin of the Pétérey torrent and others at the origin of the glacier are taken as points of reference in order to quantify also, in an approximate way, their displacement.



*Figure 13 : Location of the blocks under analysis in Bonnard glacier, from Swisstopo, 2020*

With a trial and error procedure, the comparison reported here is made among different periods of time, to show the continuous advancement of the material towards the valley, which appears to occur especially in the South-West direction. Not only sliding is visible, but also the rotation of blocks, the glacier's rheology and its roughness changes.

The first result is about the longest period taken into consideration, that is 13 years, between 2007 and 2020: in *Figure 14*, red circles highlight changes of position of some boulders which appears to be quite evident.

Taking advantage of *QGIS* software, measurements have been done: the bigger and upper rock (n°1) moved around 12 m, while the smaller below (n° 2) around 7 m, meaning an average advancement rate of 0.5-0.9 m per year.



*Figure 14 : Displacement during the period 2007-2020 of the rocks 1 and 2*

The second period taken as an example is 2010-2016: in this case, another rock is considered and from left to right, the movements result to be around 6 m, 3.5 m and 4 m. The first two blocks show a motion which is more or less half of the one obtained in the previous case, as well as the time lapse, meaning that the rate remains stable around 0.5-1 m per year.



*Figure 15 : Displacement during the period 2010-2016 of three rocks*

It is interesting to note that, trying to compare two-time intervals each one of three years, the displacements of the considered material result to be greater in the recent period: between 2007 and 2010, the boulders n°1 and n°2 move respectively 2.7 m and 3 m, while between 2017 and 2020, the same ones, move 4 m and 3.5 m, showing an overall acceleration. In this case, images are not displayed because the motion is not significantly evident to the naked eye.

At this initial stage, without any further kind of data, it can be affirmed, from the theory (R. Kenner, 2017), that this phenomenon is mostly triggered by an increment of permafrost temperature and a consequent increment in water supply due to snow and/or ground ice melt

and also precipitation, which can explain both the frequency and the amplitude of the debris flow events.

This is what it is possible to understand by considering a preliminary and general analysis of the behaviour of temperature, in the last centuries, in the Southern part of Switzerland as shown in *Figure 16* (detailed meteorological data will be instead discussed in the next section).

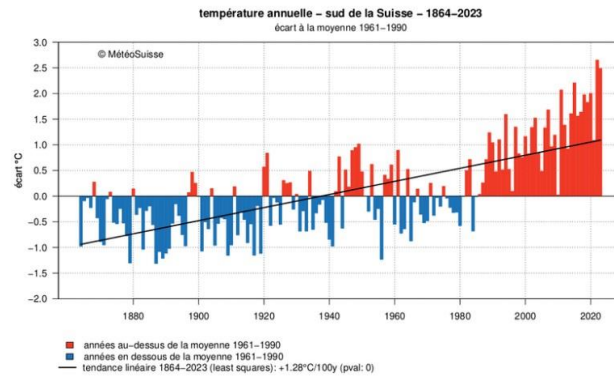


*Figure 16 : Temperature increasing trend from 1864 to 2023*



*Figure 17 : Zoom on the blue area through different years: surface's deformations are visible as time passes: a. 2007, b. 2009, c. 2010, d. 2012, e. 2014, f. 2016, g. 2017, h. 2020*

In order to better visualize and appreciate the changes detected on the surface, a photo monitoring software is exploited: *IRIS* in fact allows to quantify, starting from the images in input, the displacements of the area under analysis, considering pixels' images. This thanks to



the comparison between the so called “master”, in this case the one of 2007, and the “slaves”, namely 2010, 2012, 2013, 2017 and 2020. A colorbar helps the interpretation of the results to detect the major and the minor movements together with some arrows which underline the flow direction.

As it can be notice, throughout time, there is an intensification of the displacement because red, purple and blue colors are more and more present and widespread, meaning an overall acceleration, especially in correspondence of the two lobes of the rock glacier which are clearly visible.

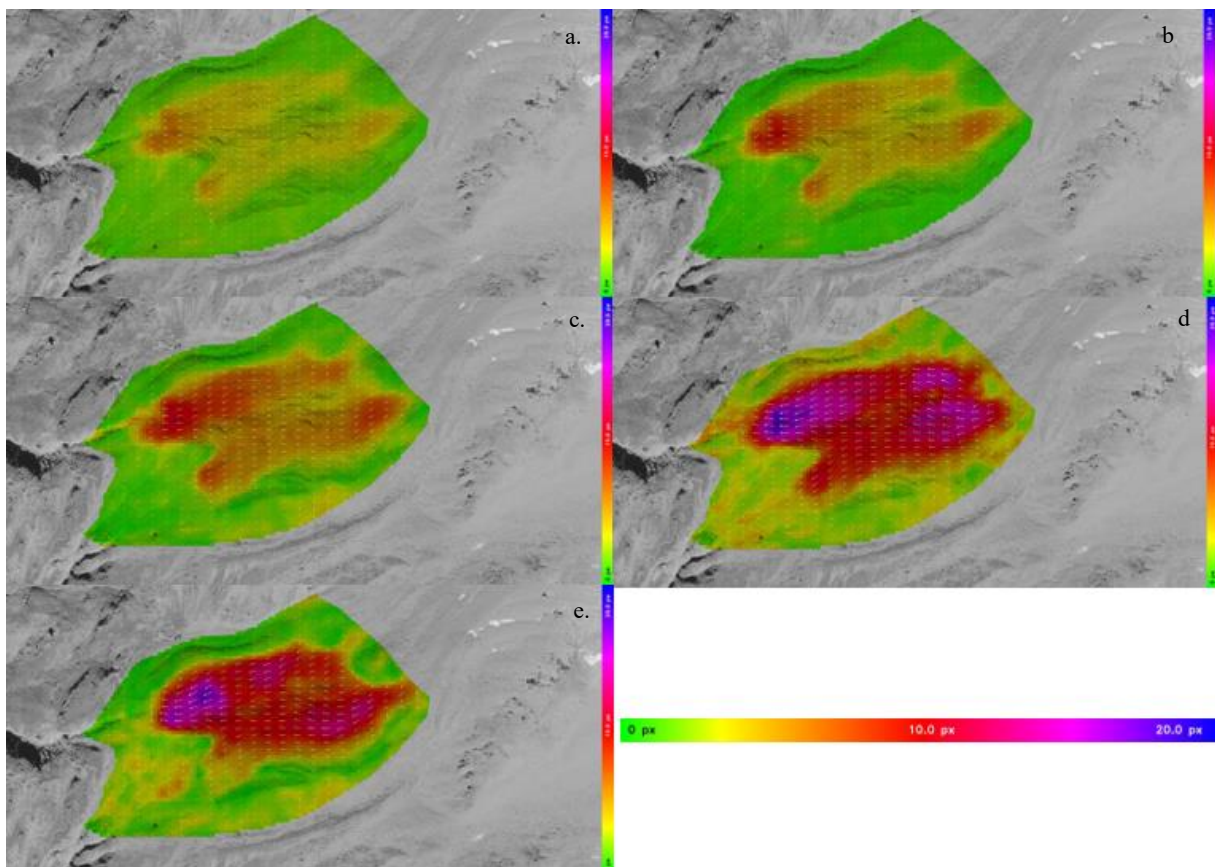


Figure 18: Displacements of the area in analysis (the one considered for the GPS – see Chapter 4.2 ) with respect to 2007: a. 2007 vs 2010; b. 2007 vs 2012; c. 2007 vs 2013; d. 2007 vs 2017; e. 2007 vs 2020.

Also focusing on the upper part of the glacier, it is evident that the quantity of debris has enlarged through time.

Between 2007 and 2010, a new boulder appears and it is clearly visible on the image, together with some changes of the glacier's surface:



*Figure 19 : Movements on the upper part of the glacier with an highlight on the new boulder*

By following its displacement over the years, the results are roughly:

- from 2010 to 2012, 1.3 m;
- from 2012 to 2014, 1.2 m;
- from 2014 to 2017, 2.5 m;
- from 2017 to 2020, 3.2 m,

for a total sliding of around 8 m, more pronounced in the last years and so in agreement with what has been previously discussed.

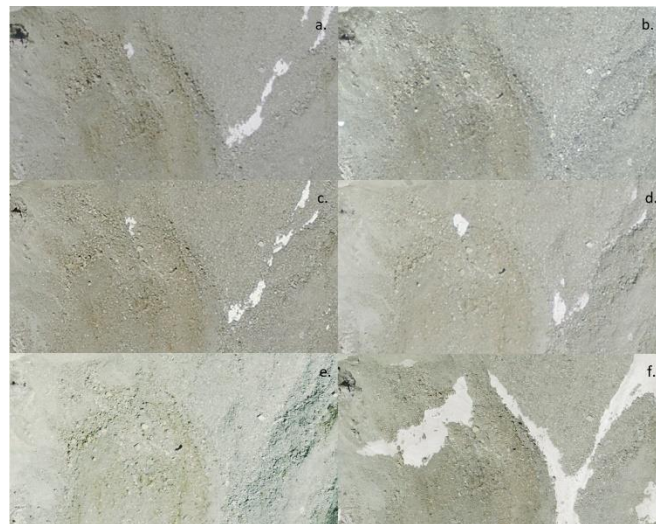


*Figure 20 : Deformations in the surface at the origin of the glacier during different years: a. 2007, b. 2010, c. 2012, d. 2014, e. 2017, f. 2020*

## 4. Chapter 4: Quantitative analysis

### 4.1 Meteorological data

Meteorological data are obtained from three automatic weather stations, two owned by MeteoSwiss, the federal office of meteorology and climatology of Switzerland and the third by IMIS, (the Intercantonal Measurement and Information System). These are the closer available for the area of interest.

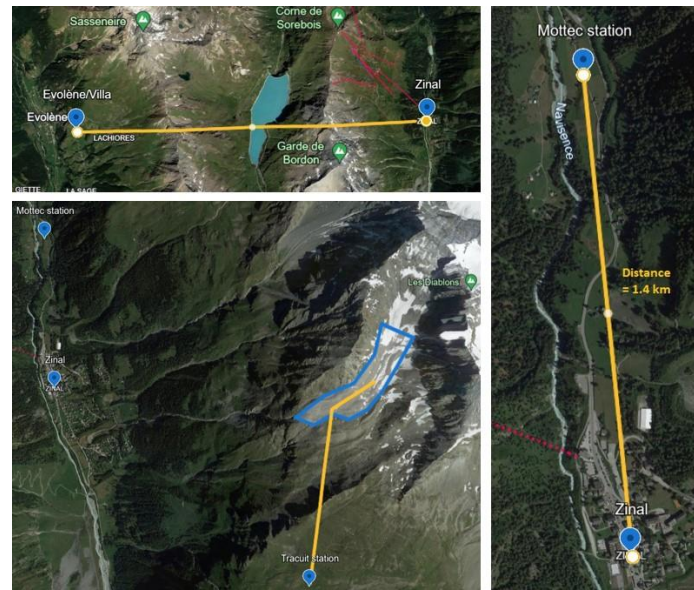


Figure 21 : The three station's location with respect to Bonnard rock glacier (blue perimeter)

The closest one is the “Mottec” station, located at 1580 m, 1.4 km upstream from Zinal, which belong to the hydroelectric plant standing in that zone: for this reason, only precipitation have been recorded during time. In any case, this kind of data is taken into account because of its relevance, knowing the important role of water and snow in the glacier's dynamic.

The other is instead the “Evolène/Villa” station at 9 km in beeline from Zinal, around 300 m higher than the village (1825 m), so still representative for temperatures' analysis.

From that, it has been possible to plot timeseries respectively for precipitation and for temperature to have an idea of the main trends occurring in that zone.

In the first case, data are available from 1973 to 2023, as monthly and annual sum, but due to the fact that GPS data (see Chapter 4) are recorded only from 2007, in order to be coherent with them, also precipitation's trend are considered from that year.

Considering the annual value, the result is a small decrement in the average precipitation in this area: according to MeteoSwiss, in Switzerland 2007 has been very hot, sunny and also very rainy, one of the five warmest years since the first measurements were made 150 years before.

In fact, in the timeseries, this year shows the maximum precipitation value (85 mm) against an average of about 64 mm over 16 years.

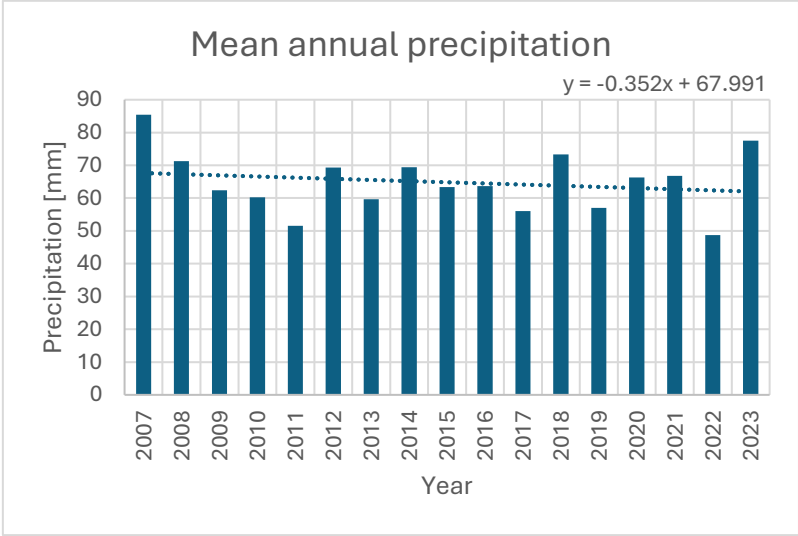


Figure 22 : Annual precipitation recorded at “Evolène” station

The minimum value has been instead recorded in 2022 with a mean of 49 mm; by considering 2007 as an outlier and so starting the series from 2008, the trend becomes positive, coherent with the current climate models: the rising in temperature (just generally commented above) is increasing evaporation and so the presence of water vapour in the atmosphere, intensifying the Earth’s water cycle.

In the specific, in Zinal, the highest precipitation was recorded in 2023 (77.5 mm) with a mean of 63.5 mm per year.

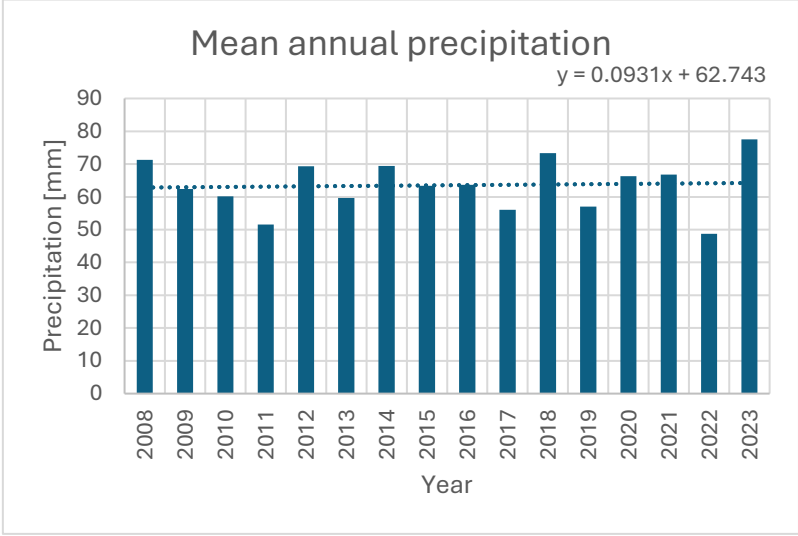


Figure 23 : Annual precipitation at “Evolène” station without considering 2007

In order to have a complete environmental overview, also temperature need to be taken into account: in line with what previously explained, but also with the global trend, they are increasing through the years, between 2007 and 2023.

Clearly, the values measured at this station are higher with respect to the ones at the Bonnard glacier, due to the difference in the elevation (at least 1500 m): knowing from the theory (MeteoSwiss, s.d.) that approximately, on average, for every 100 meters of elevation rise, the air temperature decreases by an average of 0.65 °C and knowing the mean difference in the elevation, it has been possible to estimate also the trends between 2850 and 3500 m, considering a decrement of respectively 6.5°C and 11°C.

The final timeseries are shown in *Figure 24*, with a visible positive trend of temperatures throughout the years.

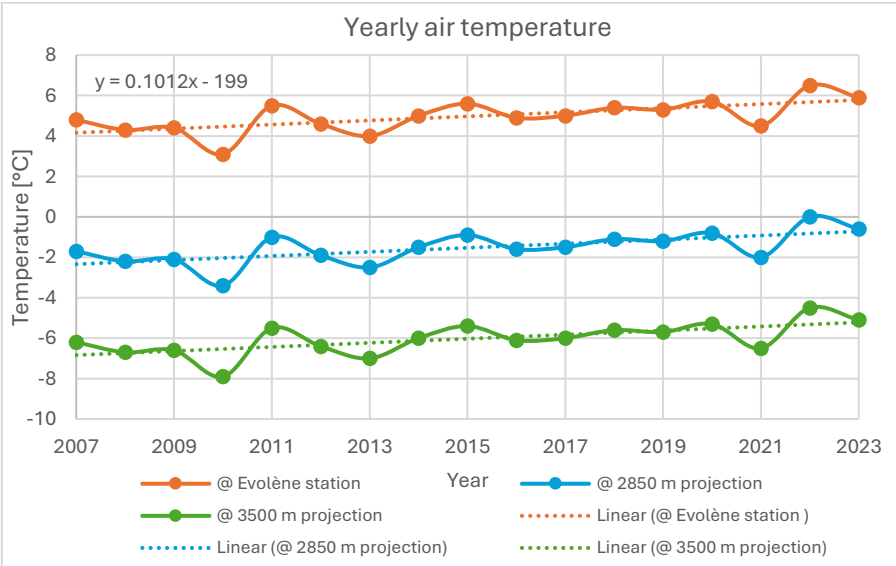


Figure 24 : Annual temperatures' trend at "Evolène" station together with a rough estimation at glacier's elevations

For a better investigation, timeseries are taken also from another automatic station, belonging to IMIS, the "Tracuit" one, at 2859 m, altitude closer to the one of interest and, in a straight line, between 1.4 and 2 km of distance.

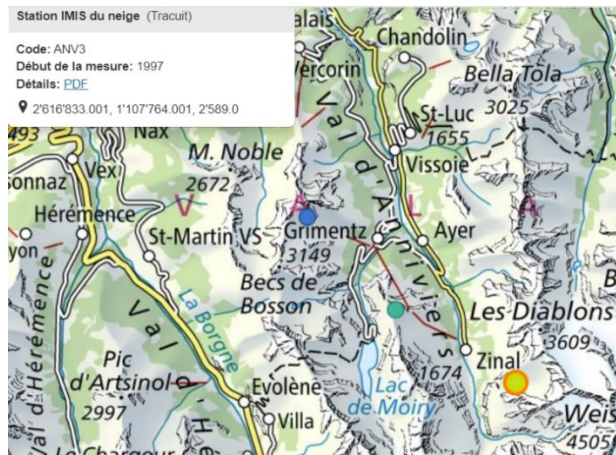


Figure 25 : « Tracuit » station's position (yellow point) with respect to Zinal, from IMIS

Relevant data result to be in the specific air temperature [°C], snowpack height [cm], snow temperature at ground and at different depths [°C], available from January 1998 until December 2023, recorded every 30 minutes for every day of the years. For that reason, daily, then monthly and annual averages have been performed in order to be able to analyse them in the proper way.

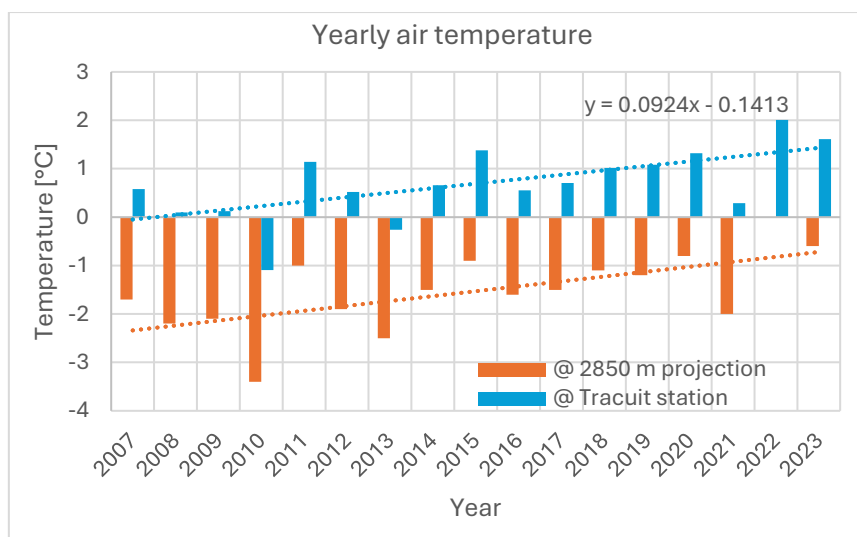


Figure 26 : Annual air temperature at Tracuit station and the projection at 2850 m

The results are from 2007 to 2023 in accordance with the precipitation and the monitoring data from GPS: mean air annual temperature shows a positive trend and are not so far from the previsions previously calculated. The delay is of about + 2°C, meaning that overall temperature even at high altitude are higher than expected and an anomaly behaviour is evident (light blue VS orange): according to the formulated hypothesis, temperature should have been for all the 16 years below the line of the zero degree, which seems to be plausible at such elevations, but instead it is not like this.

What is it possible to notice is that starting from 2014, temperature's mean values are no more below 0°C, with an average of + 1.06°C and a major value of + 2°C in 2022, indicating that the soil is certainly not frozen during all the year.

It is interesting to consider also different monthly temperature variations over the years, which show an important vertical shift, on average positive: in blue the mean trend for the first recorded year (2007) with a linear coefficient of 0.17, while for the grey one (2023) is 0.63.

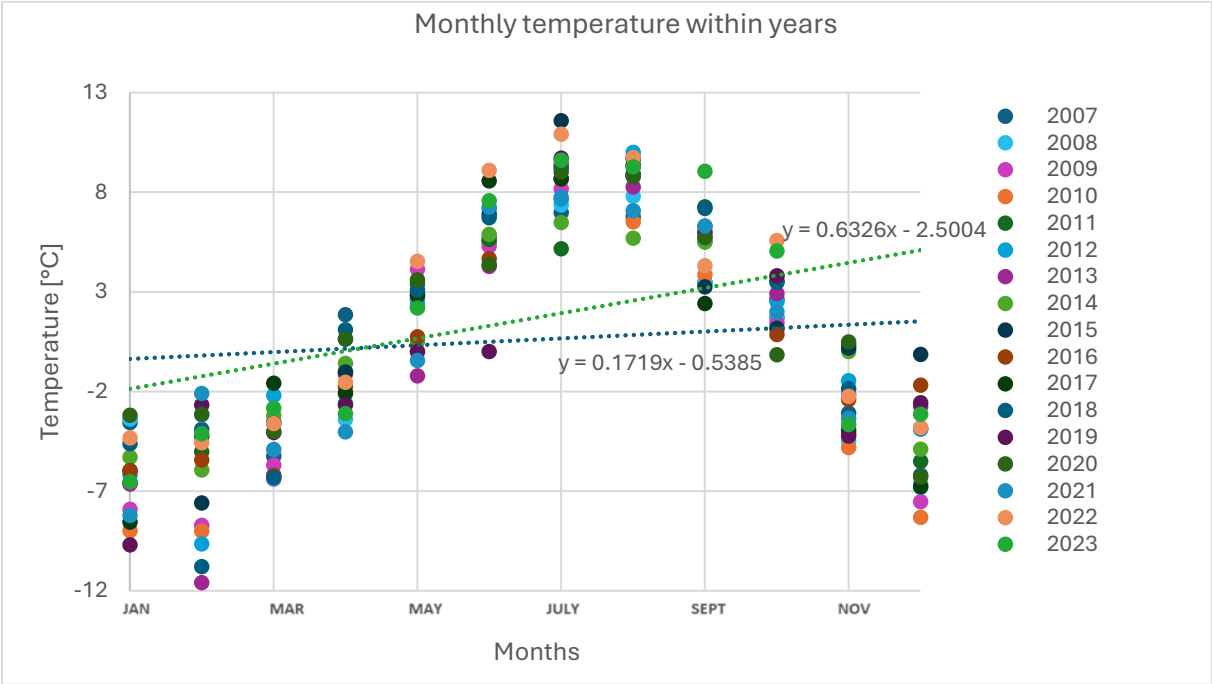
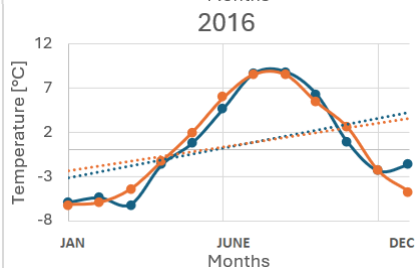
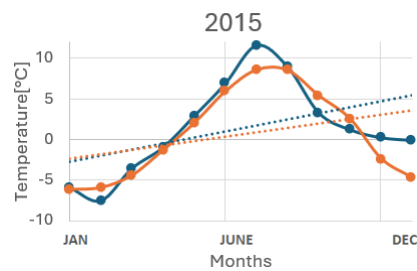
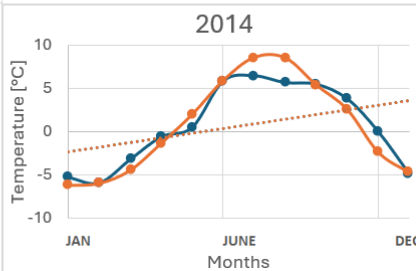
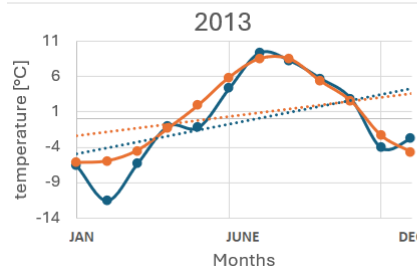
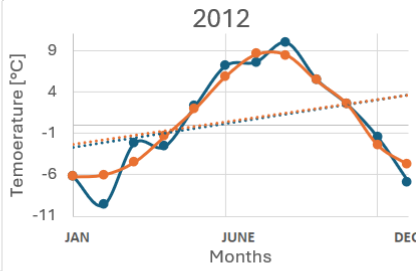
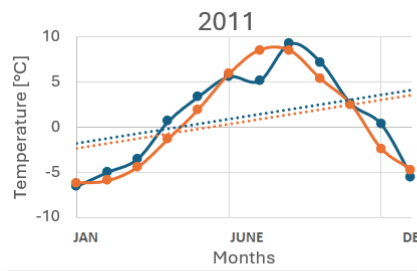
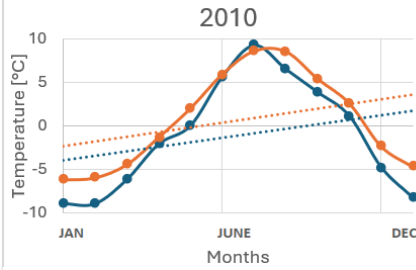
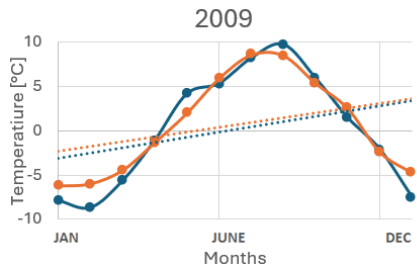
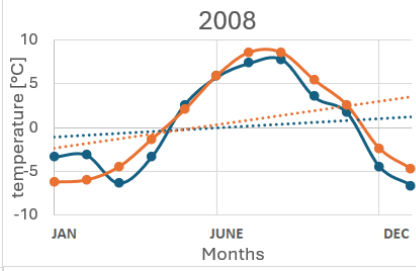
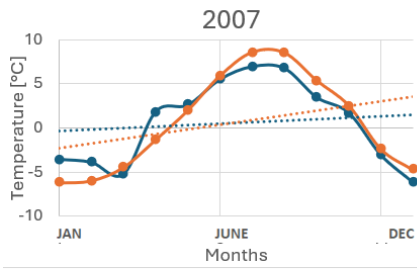


Figure 27 : Air temperature variations through years with mean trends calculated for 2007 and 2023

From the following plots in Figure 28, it is possible to appreciate that especially starting from 2015, recorded temperature result to be higher than the mean calculated over the 16 considered years, indicating an important general increment in temperature during all the months of all the years, visible also looking at the trend curve (in orange) which result to be above the blue one (which indicates the trend for the specific year).





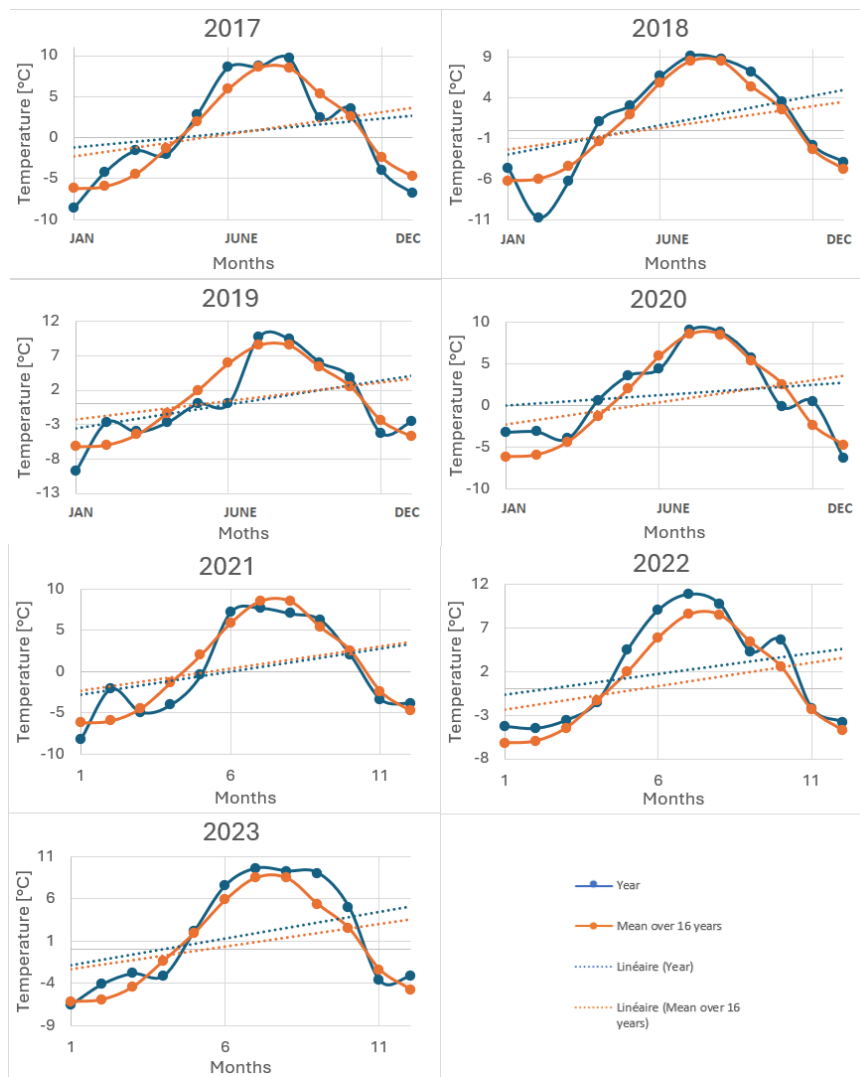


Figure 28 : Monthly temperature per year with respect to the mean over the considered period

At this point, an important consideration can be made: both precipitation and temperature data have been taken into account because of their important contribution to the energy fluxes at the surface and to thermal characteristics of the active layer of the rock glacier, in terms of growth, degrowth and maintenance. In fact, snow cover changes must be considered for their role of insulating the ground (from the cold air during winter and from warm one in summer) and of influencing the surface albedo (W. Haeberli B. H., 2006). This is related to the phenomenon called “positive feedback” which is happening everywhere in the Alps: higher temperature means less snow because of higher rates of snowmelt which means a decrement of the albedo, so lower reflectance and more absorption which brings to a warming of the ground, with a continuous cycle.

Moreover:

- when a thick snow cover exists on rock glaciers (typical of winter periods), active layer temperatures are mainly controlled by conduction and temperature variations are smooth and follow the surface temperature with a considerable lag;
- viceversa, when a thin snow cover exists (typical of spring and summer periods), non-conductive heat transfer processes occur and surface meltwater percolates into the active layer and refreezes. Also, if warm air masses deliver rain on cold snow in winter or spring, the refreezing of percolating water can warm the snow and the upper part of the active layer appreciably.

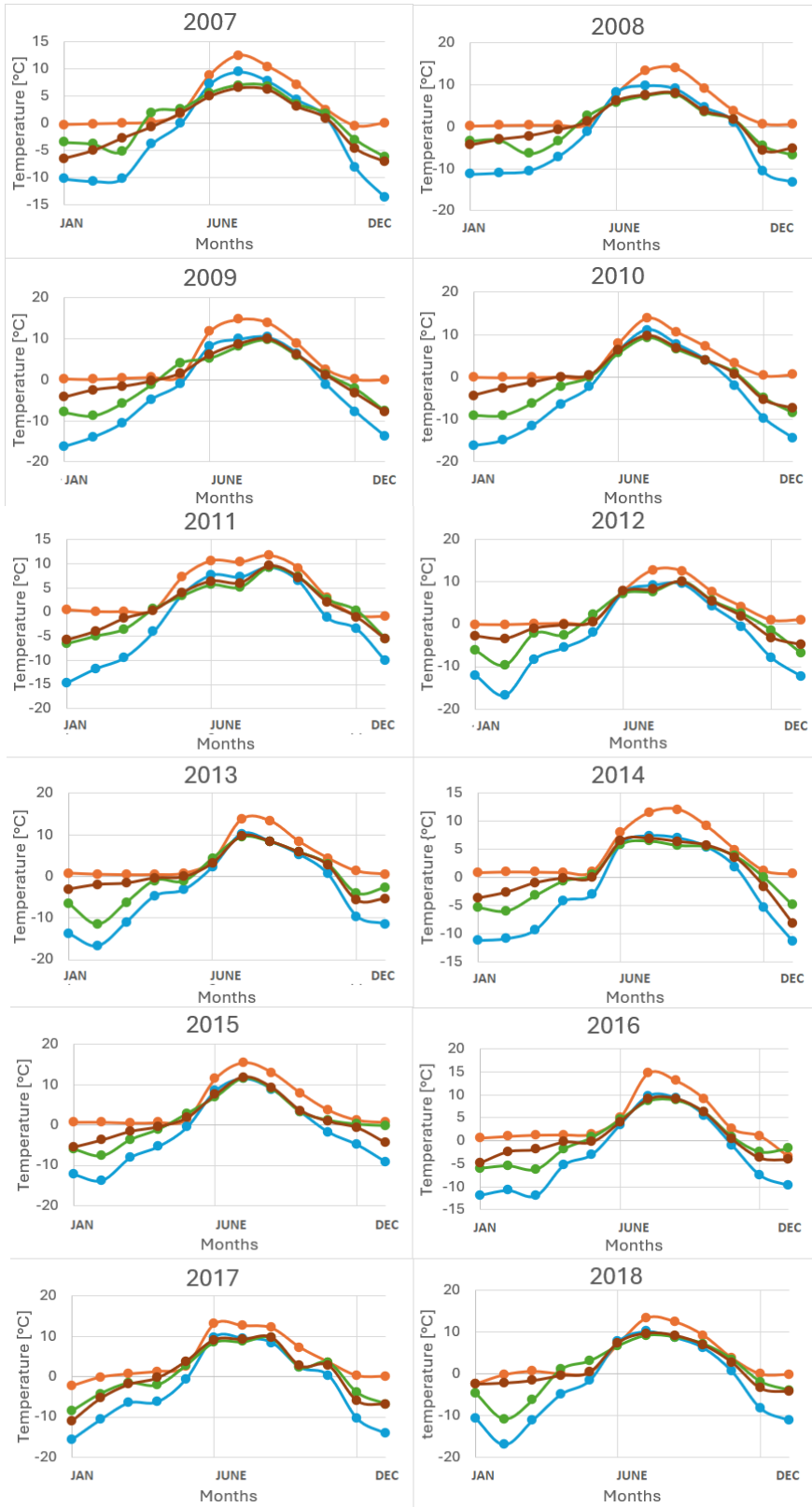
Consequently, what it is interesting is to compare air temperature, snow temperature at ground, snow surface temperature and temperature at 50 cm in depth, considered as representative for the active layer. In particular, by analysing the different layers which characterise a rock glacier from the temperature point of view, it can be said that:

- the active layer insulates permafrost from external temperature forcing and on its turn, it is influenced by freeze-thaw cycles and by the advective heat fluxes;
- for the ice-rich core, thermal regime is controlled by heat diffusion and its displacement (creep of ice) is strictly related to temperature variations;
- in the shear horizon, seasonal temperature changes are attenuated and the creep is more influenced by pore water pressure;
- in the bedrock temperature can be both positive and negative depending on the behaviour of the upper layers.

Moreover, it is known that ground surface temperature can be associated to annual variations in rock glacier surface velocities, because, due to the slow propagation of annual surface thermal anomalies, they are strictly linked with the variations of the temperature of the upper permafrost layers. It is for that reason that ground temperatures are considered “the only direct, quantitative and comparable observations of permafrost, constituting the basis of its climate-related monitoring” (J. Noetzli C. P., 2023).

Moreover, recent observations also suggest that the sensitivity of rock glaciers to climate may increase when ground temperatures approach 0°C (X. Bodin, 2009).

Following these findings, the plots in *Figure 29* can be understood:



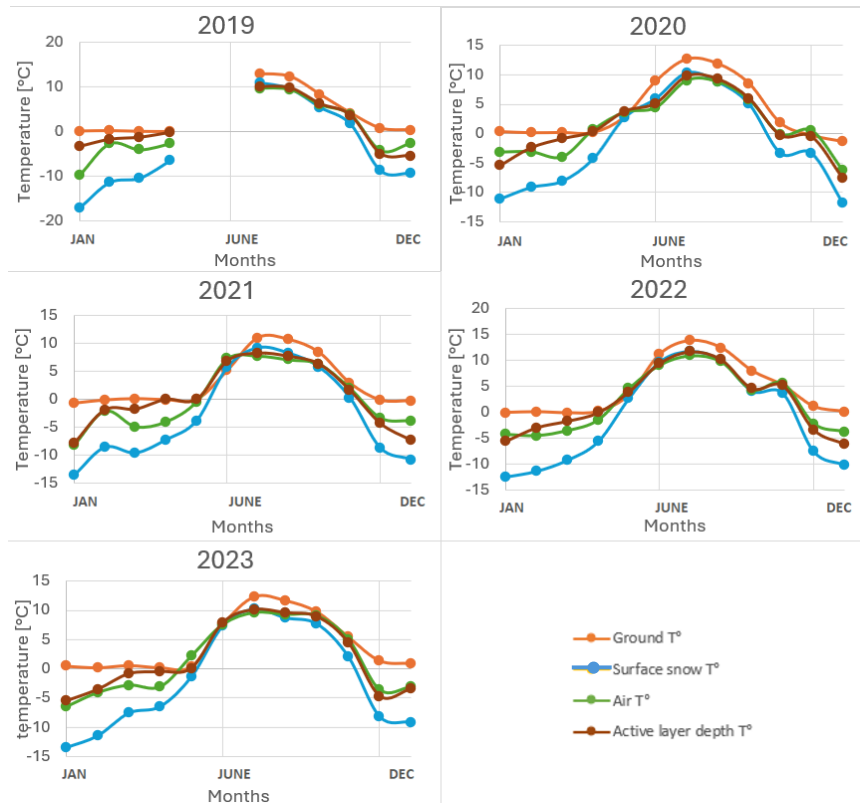


Figure 29: Monthly ground, surface snow, air and active layer temperature

It can be noted that, since 2012, from June to September, air and snow surface temperature and temperature at 50 cm of depth basically follow the same profile with respect to the other months where more or less significant lags can be appreciated.

From 2007 to 2011 instead, during summer periods, surface snow temperature are higher than the other two considered parameters.

Ground temperature, ranging between negative and positive values, are always higher than the others plotted data because of the insulation deriving from snow, rocks and debris.

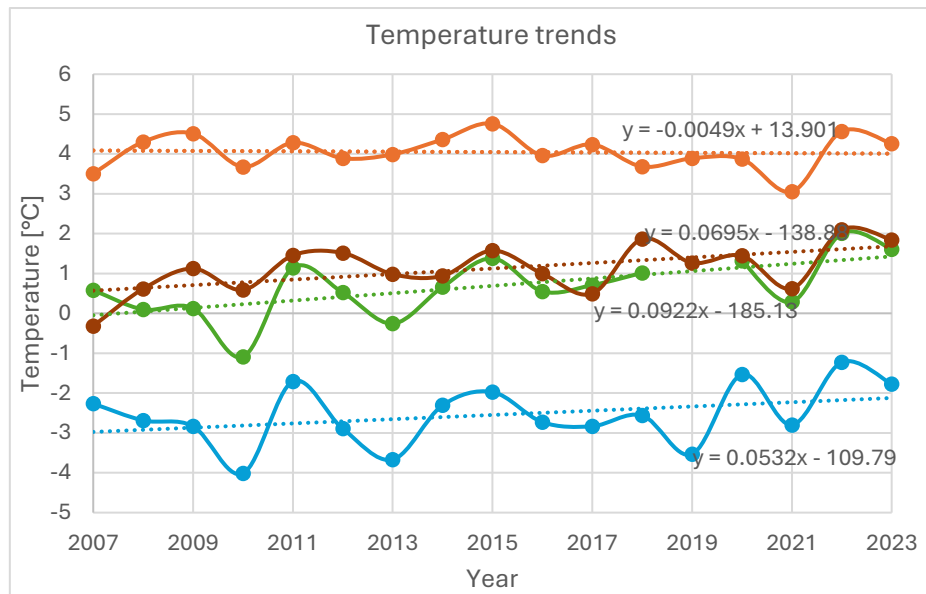


Figure 30 : Temperature trends respectively of ground, active layer, air and snow surface

By plotting the mean annual values, air temperature are the ones which increase more, with a linear coefficient of the trend curve which is the highest (0.09) and an average over the considered period of + 0.6°C, with a minimum of – 1.0°C reached in 2009 and a maximum of + 2.0°C in 2022.

The active layer temperature values are similar to the previous ones, especially during the very recent years, when they can be considered practically identical. This can be associated to a decrement of the snow cover, as it will be show later, meaning lower insulation. With an average of + 1.1°C, the minimum was recorded in 2007 with – 0.3°C while the maximum in 2022 with + 2.1°C.

Even if until nowadays snow surface temperature remain always below 0°C (mean of – 2.5°C) their trend is increasing, while as expected, ground temperature are the highest (mean of + 4.0°C) with a not significant trend through time, the only one that hardly not decreases and that can be considered as stable. This is because the response of the system is delayed in time: in 16 years it is not possible to already see the effects of the important increment of the air temperature, which can be surely, unfortunately, appreciate in a few years.

At this point, another fundamental question to address is: which kind of precipitation are occurring in the area of interest? Liquid one (rain) or solid one (snow)? This is a crucial aspect because they clearly involve different impacts on the glacier. Permafrost creep depends both on temperature variations, which affect mostly the ice viscosity, and on pore water pressure (R. Delaloye C. L.-R., 2010). In the specific, on one side, once it has reached the soil, water follows two possible paths:

- the infiltration, if it can enter the soil, moving between rocks and debris;

- the runoff, if it flows across the surface of the land.

In this way, the flow can be above, through or below permafrost, as shown in *Figure 31*:

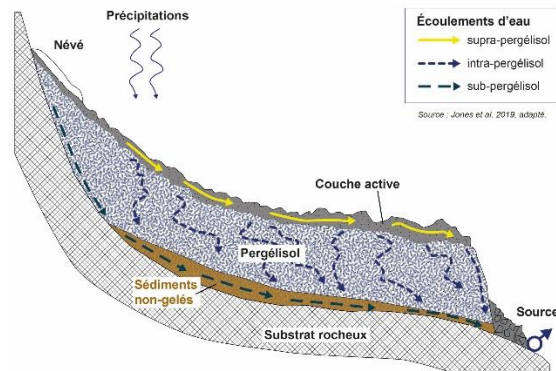


*Figure 31 : Simplified model of hydrological functioning of a rock glacier, with possible precipitation paths*

The first case is an important cause of instability: water flows in the interstitial spaces and, due to changes in temperature between day and night and/or between seasons, cracks into rocks which inevitably move more.

The second, instead, allows water to flow far away from its falling points and to reach other zones where perhaps it can infiltrate, creating in such a way the same aforementioned scenario. But precipitation data are available, as just seen, only at 1500 m and not at the elevations of interest (more than 1000 m above): a possible hypothesis has been formulated starting from precipitation and air temperature values (for both the one of “Evolène” and of “Tracuit” stations): firstly, the estimation has been conducted at around 1500-1800 m in the area of Zinal, thanks to precipitation data coming from “Mottec” station and to temperature ones coming from “Evolène” station; then, the same reasoning was followed for “Tracuit” temperature data.

The principal encountered difficulty is that the snowfall limit is not a sharply-defined line; in general, several hundred metres deep (below the zero-degree level) snow crystals gradually give way to raindrops and consequently the snowfall limit is always lower than the zero-degree level. It can be assumed that snow commonly occurs 200 to 400 metres below the zero-degree level (MeteoSwiss, s.d.).

So, temperature from “Evolène” station have been taken into account and then, considering what just explained, calculated for 300 m (an average between 200 and 400 m) below with a consequent increment of 1.95°C (for the rule described above for temperature’s projection). With a gap of 0.1°C, all temperature recorded in “Evolène”, resulting to be lower than this value, have been associated to solid precipitation, namely snow. In such a way, it results that rainfall occur generally more than snowfall at this elevation, as shown in the following pie chart.

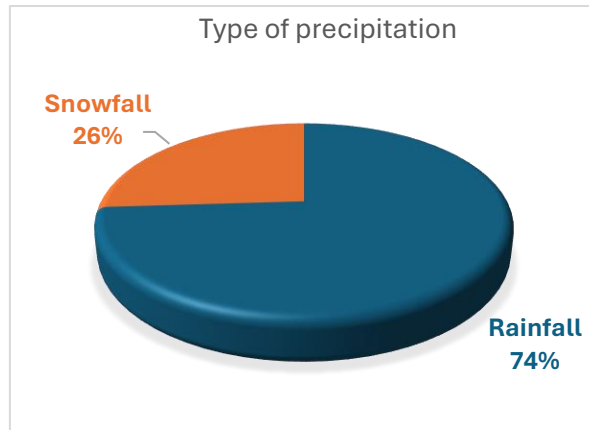


Figure 32 : Precipitation typology at “Evolène” station between 2007 and 2023

Then, also the total annual amount of snow has been calculated: knowing precipitation given in mm and assuming that 1 mm of rain is equivalent to 1 cm of snow (MeteoSwiss, s.d.), the result is quickly obtained: an important negative trend indicates that at these altitudes, snow is less and less present through time.

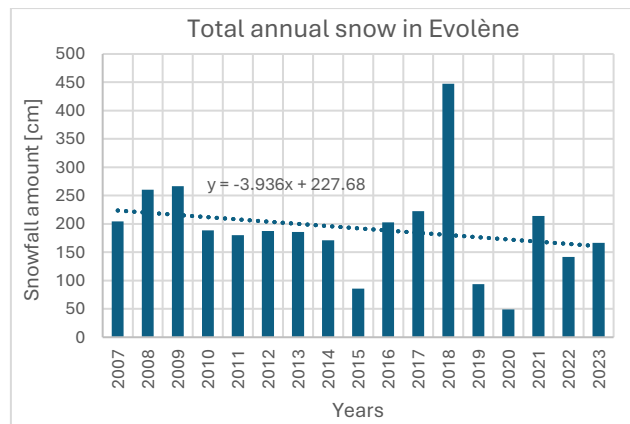


Figure 33 : Annual snowfall recorded at “Evolène” station

For the sake of completeness, also the estimated values of snowfall are reported in the following table:

Year	Snowfall [cm]
2007	204.5
2008	260.4
2009	266.6
2010	188.4
2011	180
2012	187.5
2013	186.1
2014	171.4
2015	85.6
2016	202.5
2017	222.8
2018	447.3

<b>2019</b>	93.5
<b>2020</b>	49.2
<b>2021</b>	214.2
<b>2022</b>	141.8
<b>2023</b>	166.6

Table 1 : Total snowfall for each year in analysis at “Evolène” station

Exactly the same procedure was followed for temperature values recorded at “Tracuit” station, which are the closer for the analysis of the dynamics related the Bonnard glacier.

As expected, due to the fact that the station is located at a higher elevation, over the period of the 16 years, the majority of precipitation are solid:

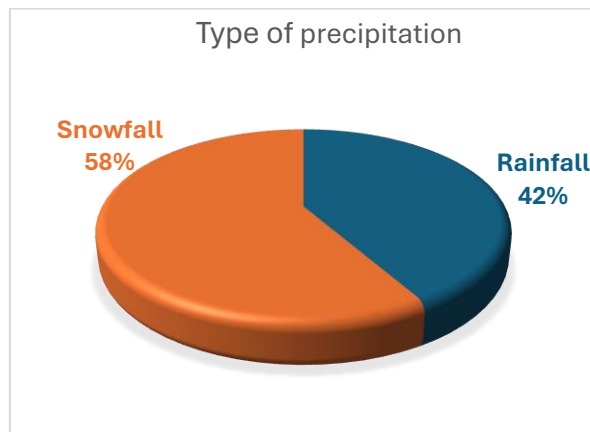


Figure 34 : Precipitation typology at “Tracuit” station

Again, the total annual snowfall was calculated, obtaining also in this case a negative trend for the solid precipitation.

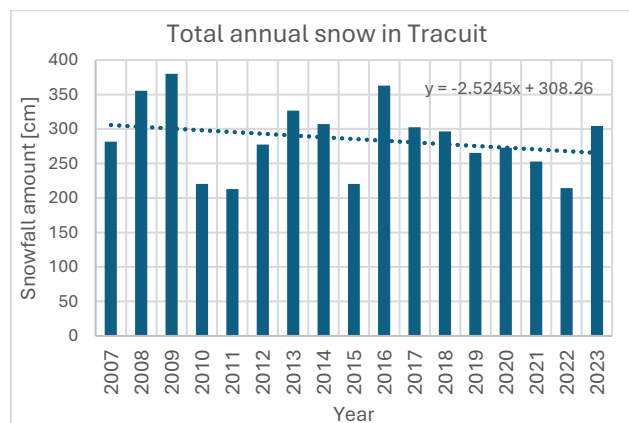


Figure 35 : Annual snowfall recorded at “Tracuit” station

<b>Year</b>	<b>Snowfall [cm]</b>
<b>2007</b>	281.6
<b>2008</b>	355.6
<b>2009</b>	379.8
<b>2010</b>	220.6
<b>2011</b>	212.8
<b>2012</b>	277.5



<b>2013</b>	326.7
<b>2014</b>	307.3
<b>2015</b>	220.2
<b>2016</b>	362.7
<b>2017</b>	302.6
<b>2018</b>	296.4
<b>2019</b>	265.6
<b>2020</b>	272.8
<b>2021</b>	253
<b>2022</b>	214.5
<b>2023</b>	304.4

Table 2 : Total snowfall for each year in analysis at “Tracuit” station

These results are in accordance with another parameter recorded at the station in question: the snowpack height. From 2007 to 2023 the mean trend of annual snow cover is decreasing, with a minimum reached in 2017 (around 25 cm).

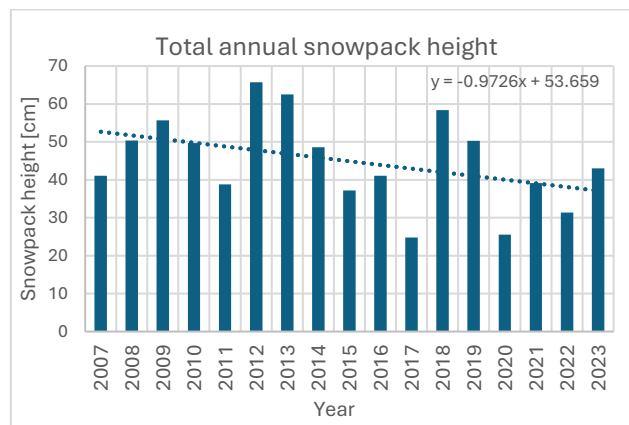


Figure 36 : Annual snowpack height

All the results are coherent: rise of temperature, reduction in solid precipitation with the consequent increment of the liquid ones and reduction of snowpack height during the period under analysis are affecting in an irreversible way the behaviour of the rock glacier. In the following graph, the visual comparison: while the snowfall amount is in rapidly decrease through the years, the snowpack decreases in a smoother way because its existence is strictly dependent not only on temperature but also on precipitation, wind, solar radiation which vary differently between day and night, between seasons and between years.

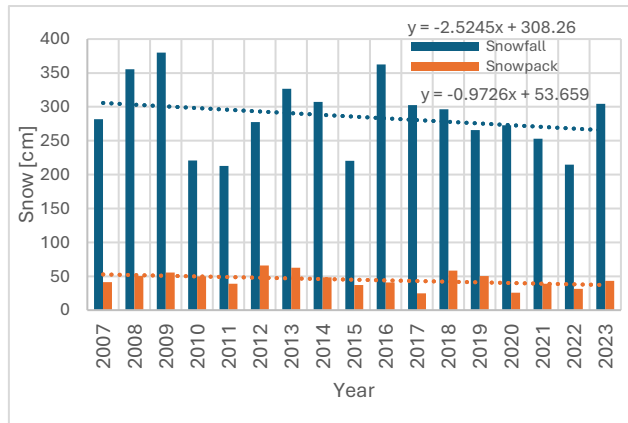


Figure 37 : Trends of annual snowfall and snowpack

## 4.2 GPS system preview

Now that the most relevant environmental data have been taken into account, it is time to move on, considering data of the monitoring carried out directly on the glacier. Together with the georeferenced time-lapse photography, in fact, surface's movements of the Bonnard rock glacier are acquired also with an in situ Global Positioning System (GPS), made with a Global Navigation Satellite System (GNSS), in RTK, the real-time kinematic positioning, namely the application of surveying to correct common errors while using GNSS, in a base-rover configuration to allow differential positioning. Consequently, the degree of precision is of 1-3 cm in planimetry and 2-5 cm in altimetry (E. Bardou G. F.-B., 2015).

The measured points were marked on the ground and data are available from 2007 until 2018, when monitoring activities ended; some points have been added through time for a better investigation of movements and deformations and some others removed because of the multiple logistic constraints on the field for which, for certain periods, not all the points could be measured, resulting in a degraded network (E. Bardou G. F.-B., 2015).

<b>Campaign date</b>	<b>Number of GPS points</b>
<b>06.09.2007</b>	123
<b>10.11.2008</b>	146
<b>09.10.2009</b>	198
<b>28.09.2010</b>	199
<b>28.10.2011</b>	216
<b>23.10.2012</b>	219
<b>06.11.2015</b>	178
<b>28.10.2016</b>	180
<b>18.10.2017</b>	182
<b>20.09.2018</b>	188

*Table 3 : GPS points on the different campaigns*

The most important information that it is possible to exploit are their coordinates X, Y, and Z, acquired in the coordinate reference system CH1903/LV03, in particular, in two ways: the first is to quantify their motion and the second is to calculate the true depth of the glacier's mass by considering as reference surface the bedrock's roof, which is the solid rock beneath surface materials (soil and gravel) where the velocity is equal to zero (so considered as stable), through time.

Finally, the major displacements are related to external climatic factors rather than the internal ones (R. Delaloye C. L.-R., 2010).

### 4.3 Slope analysis

This bedrock's roof model has been created from the monitoring activity between years 2010 and 2014 using the seismic refraction method. Specifically, different drillings have been performed to better observe the terrain, then those data, together with a topographic analysis, allowed to create the final 3D model. It gives the information about the altitude of the analysed area, the one more subject to important movements: it ranges from 2700 to 3100 m.

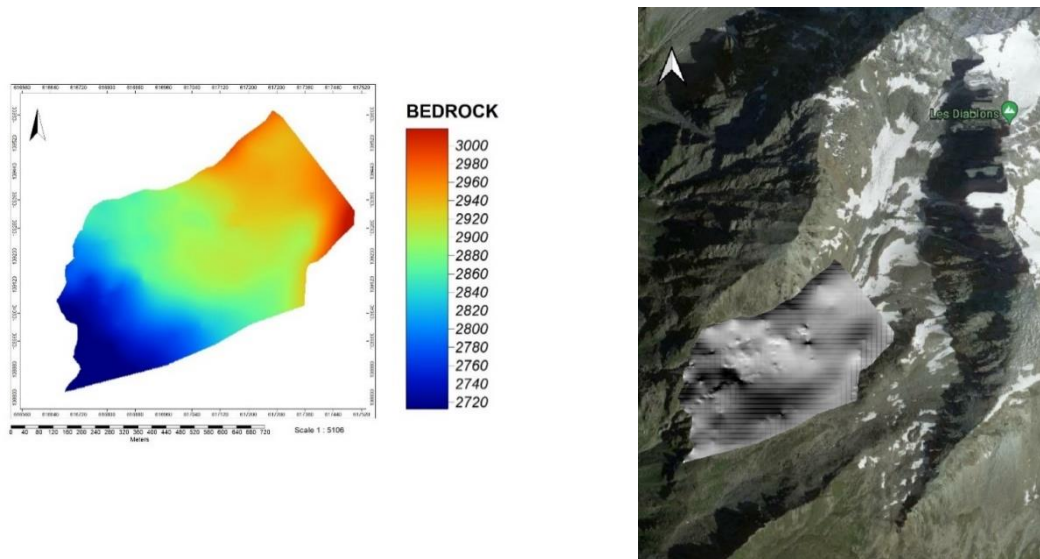


Figure 38 : Bedrock's roof, visualization in SAGA software and its location with respect to the hill, displayed in QGIS software

Then, to understand the morphometry of the area under analysis, the most important local terrain parameters of this surface have been calculated through SAGA software, namely:

- the slope, which is the steepness or the degree of incline of a surface;
- the aspect, which is the orientation of the slope, measured clockwise (from  $0^\circ$  corresponding to North to  $180^\circ$  corresponding to South, passing through  $90^\circ$  which is East and  $270^\circ$  which is West);
- the plan curvature, which is the perpendicular to the direction of the maximum slope: a positive value indicates that the surface is convex with respect to the hill, while a negative one that it is concave. A zero value indicates a linear surface (no curvature); (ArcGIS Pro, s.d.)

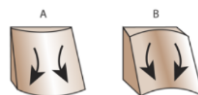


Figure 39 : The plan curvature A. convex surface, B. concave surface

- the profile curvature, which is the curvature of the surface in the direction of gradient, parallel to the slope and indicates the direction of maximum slope. A negative value

indicates that the surface is convex with respect to the hill, while a positive one that the surface is concave. A value of zero indicates that the surface is linear.

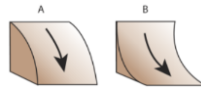


Figure 40 : The profile curvature : A. convex surface, B. concave surface

From that, it logically goes to say that plan and profile curvature give the same information, affecting the acceleration and deceleration of flow across the surface: when the surface is convex, the flow of water or of material will be decelerated, on the contrary when it is concave, the flow will be accelerated.

Starting from the slope, it is calculated that values range from about  $0^\circ$  to  $47^\circ$ ; it is noted a major inclination on the bottom of the right edge and in the middle-lower part, more visible from the 3D view which allows to better visualize the shape of the hillside.

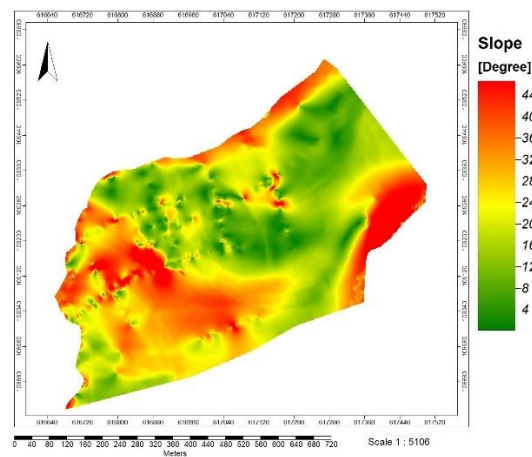


Figure 41 : Slope of bedrock's roof, 2D visualization in SAGA

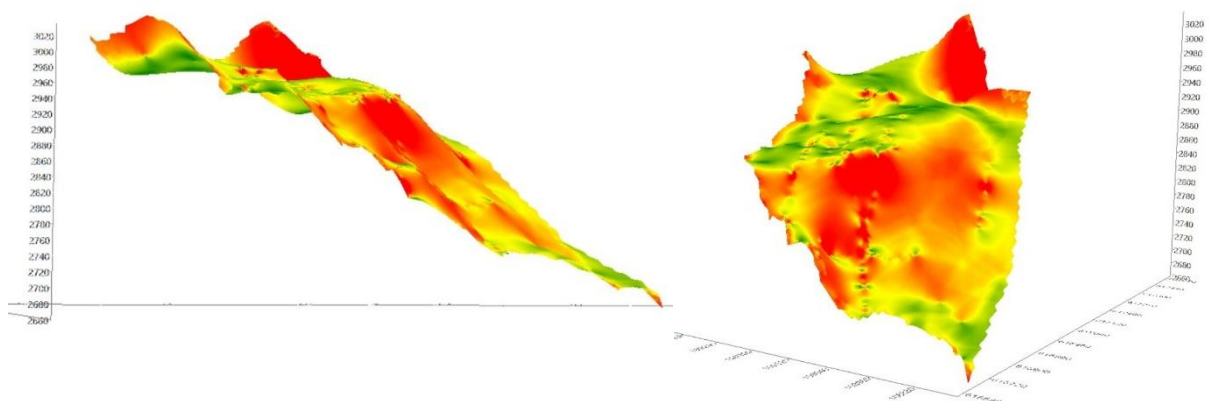


Figure 42 : 3D view of slope parameter

Moving to the aspect parameter, the calculated results go from  $105^{\circ}$  to  $330^{\circ}$  which is related to a South-West orientation of the slope.

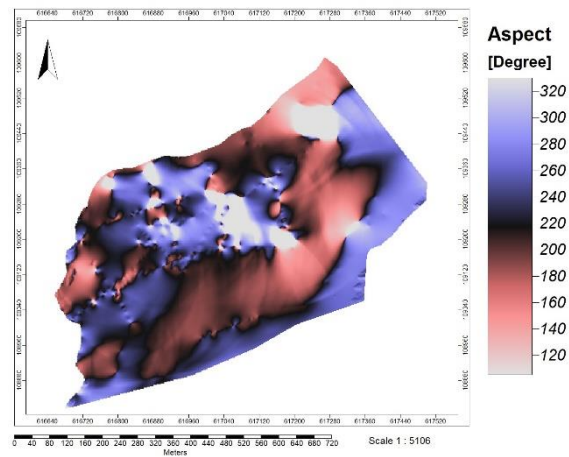


Figure 43 : Aspect of bedrock's roof, 2D visualization in SAGA

Lastly, profile and plan curvature are shown in the following: they result to be in accordance having more or less on the same positions positive values, the first parameter, and negative ones, the second and vice versa.

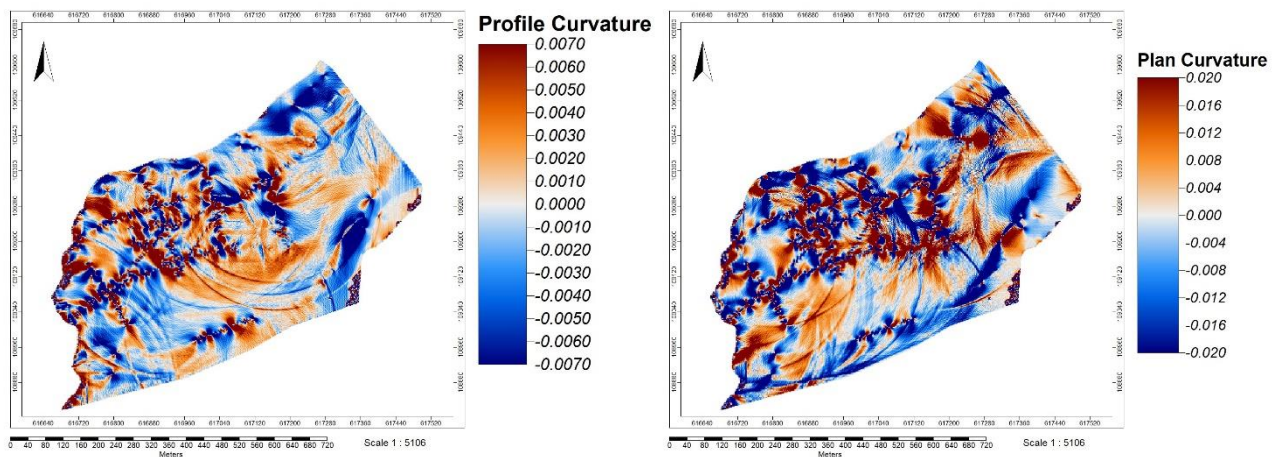


Figure 44 : Profile and Plan curvature of bedrock's roof, 2D visualization in SAGA

With a view to deep understand the morphology of the site, it was taken into account also the digital elevation model (DEM), the numerical model of the bottom, which describes the surface of Switzerland without vegetation and development, the “swissALTI3D”, again from Swisstopo website. Data are available in .TIFF format, with a resolution of 0.5 m and in the LV95 LN02 coordinate system, divided into spatial units. In total, four of them were downloaded and merged in order to cover the area of the Bonnard glacier; then, to be able to work in the same coordinate system, a transformation action was performed (so to CH1903/LV03 one).

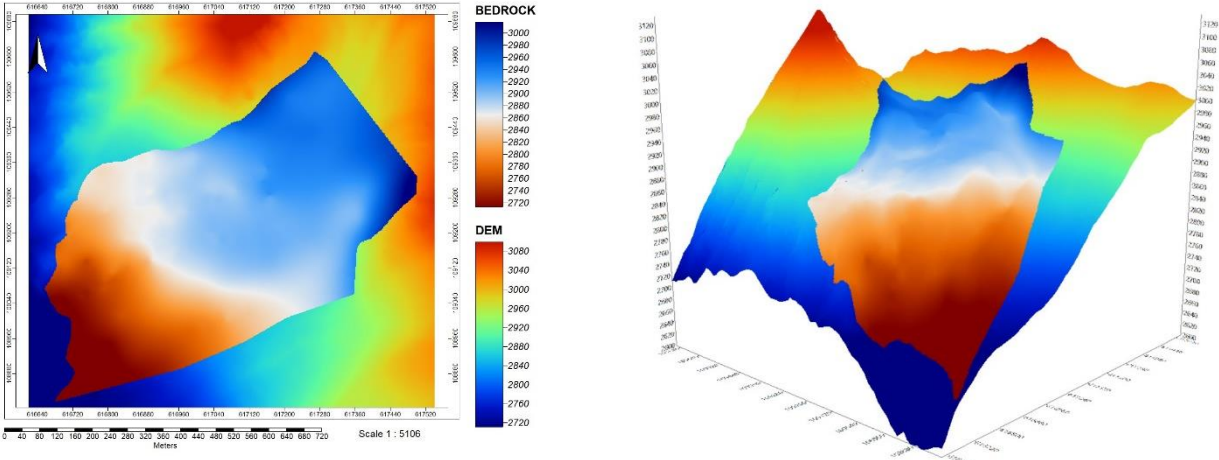


Figure 45 a. 2D view of the bedrock's roof on the numerical model (DEM), b. 3D view, in SAGA.

In particular, the objective is to understand which are the main differences between the bottom of the surface and the bedrock's roof again in term of slope, aspect, plan and profile curvature. First of all, the results regarding these parameters are shown in the following, as it was done previously. Starting from the slope, values range from about 4° to 54°:

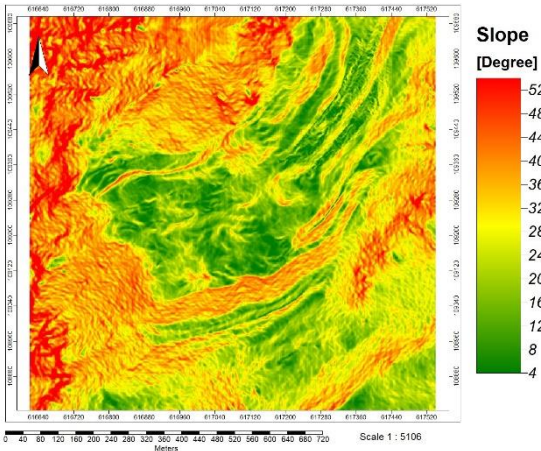


Figure 46 : DEM's slope

Aspect's values between 140° and 340° are in accordance with the one of the bedrock, indicating a surface with a mean orientation towards South-West:

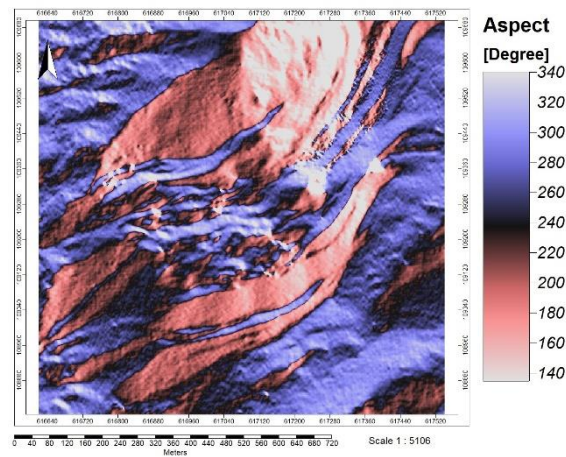


Figure 47 : DEM's aspect

Actually, again profile and plan curvature indicate the same:

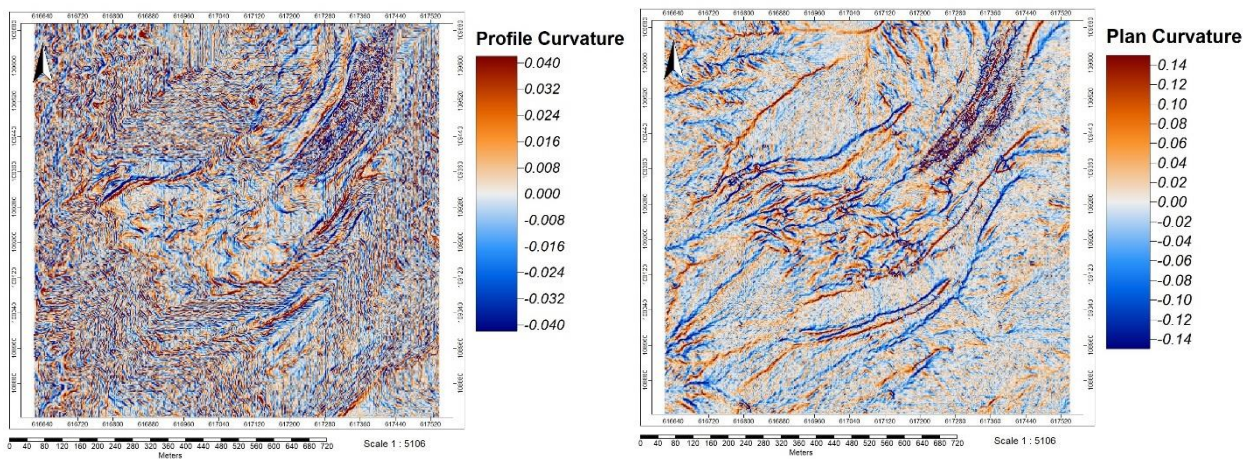


Figure 48 : DEM's profile and plan curvature

From the previous images, it is quite evident how the surfaces differ the one from the other, but to highlight more their different characteristics, taking advantage of SAGA software, the tool “difference between grid” is exploited in order to obtain, as results, changes in the elevation and in all the morphometric parameters under study, in a quantitative way.

Above all, difference is computed in terms of elevation, to figure out surface's behaviour: values range from 0 m to 40 m and to better picture the results, both following calculi were implemented:

- *DEM elevation – BEDROCK elevation:*



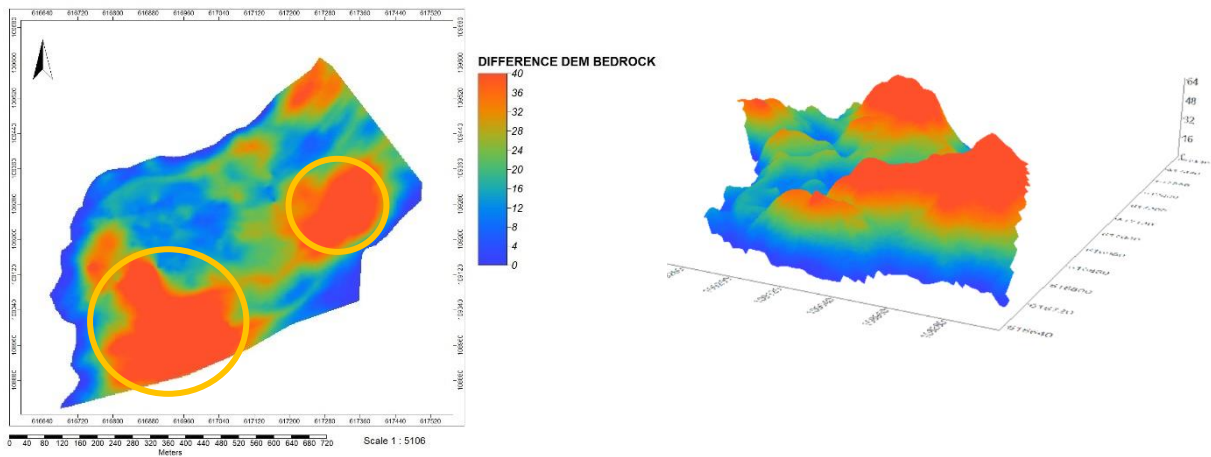


Figure 49: Elevation difference in 2D and in 3D visualization

- *BEDROCK elevation – DEM elevation:*

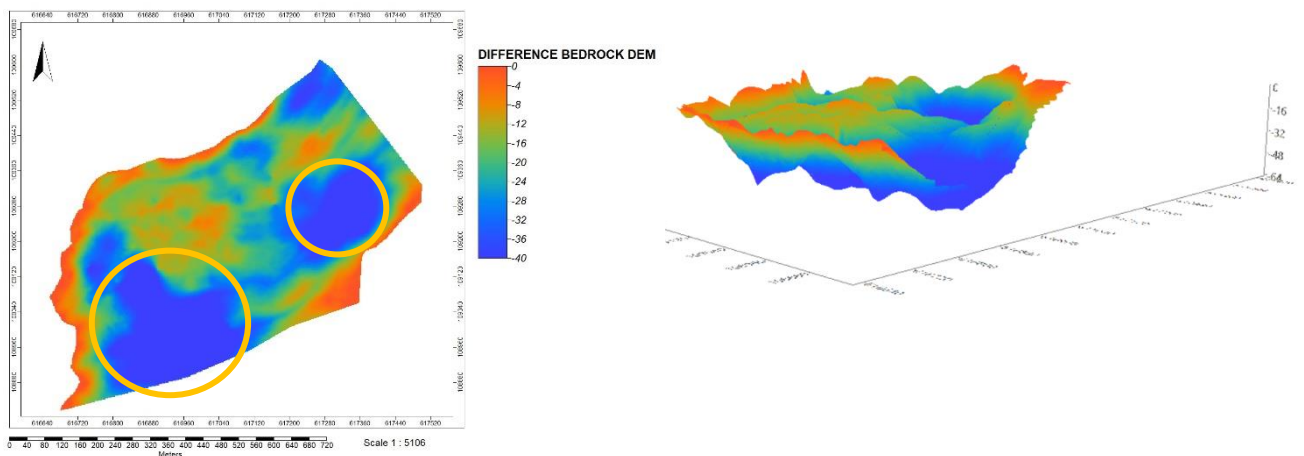


Figure 50 : Elevation difference in 2D and in 3D visualization

It is clear that the two circled zones are the ones in which bedrock's elevation is lower than the bottom one.

Moving to the slope, knowing that, from the analysis carried out above, in the area of interest the slope of the bedrock is in general higher, the difference is performed between these values and the ones of the bottom; red parts, mostly localized in the upper right part and in the middle-lower one, indicate that the bedrock is steeper than the bottom itself. This statement can be easily understood by looking at the 3D view.

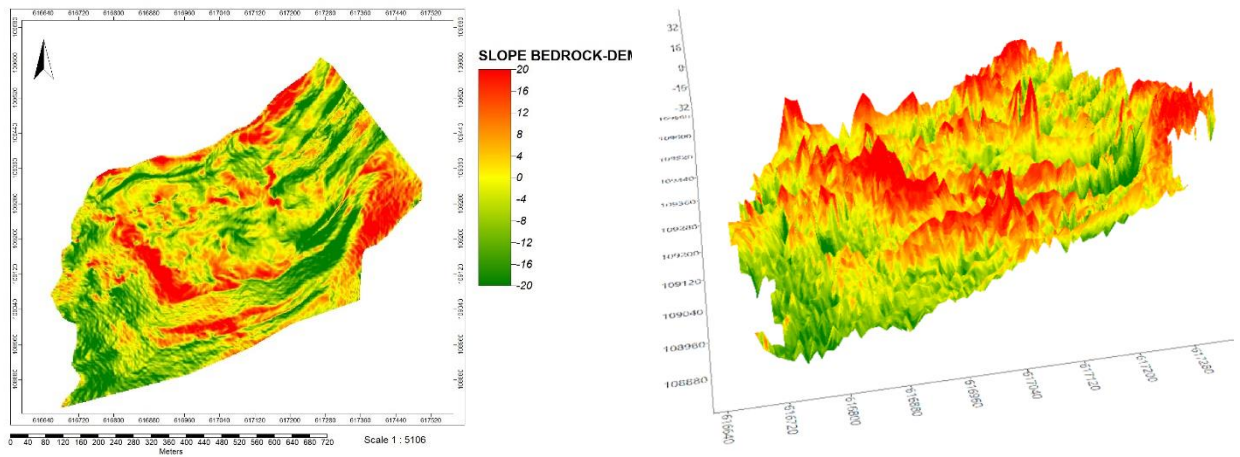


Figure 51 : Slope difference in 2D and in 3D visualization

Difference in the aspect parameter shows that the changes in the orientation remain around 30° of discrepancy meaning that, as already underline, the surfaces are virtually oriented in the same way.

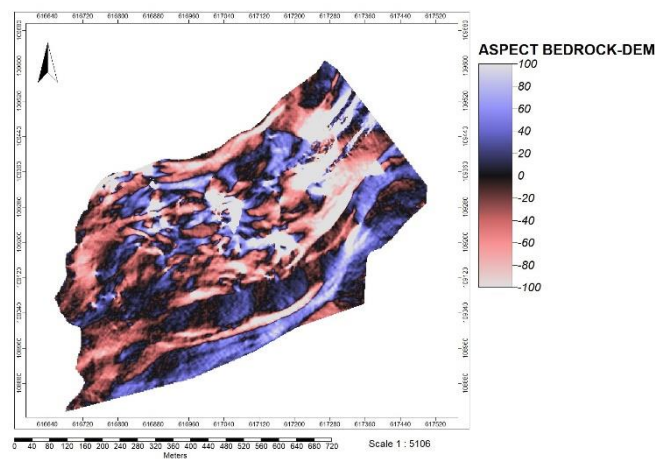


Figure 52 : Aspect difference

Profile and plan curvature differences are quite difficult to be interpreted because lots of colours are present in the results: for the sake of completeness they are put in the following:

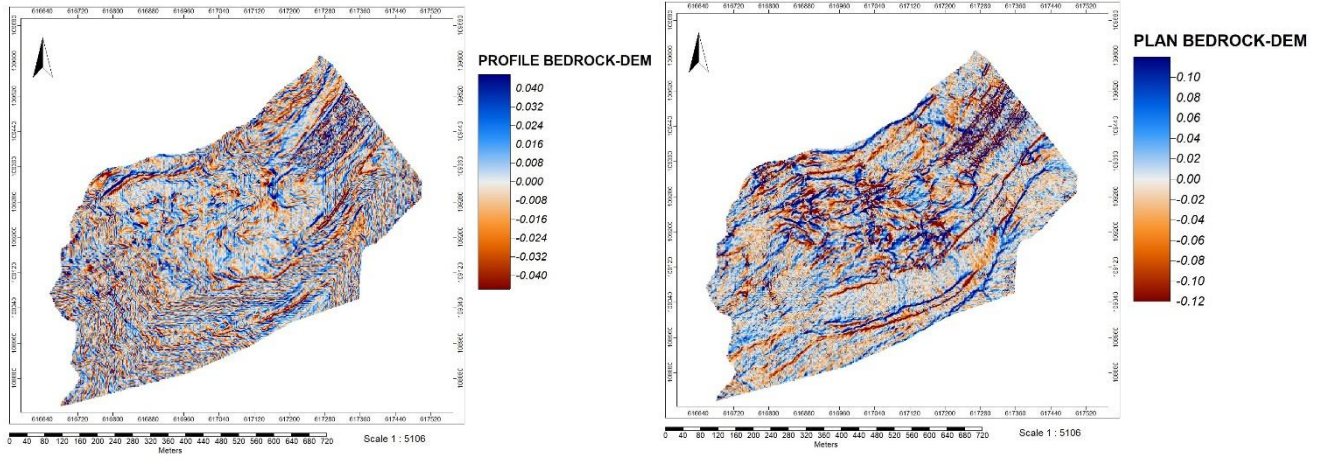
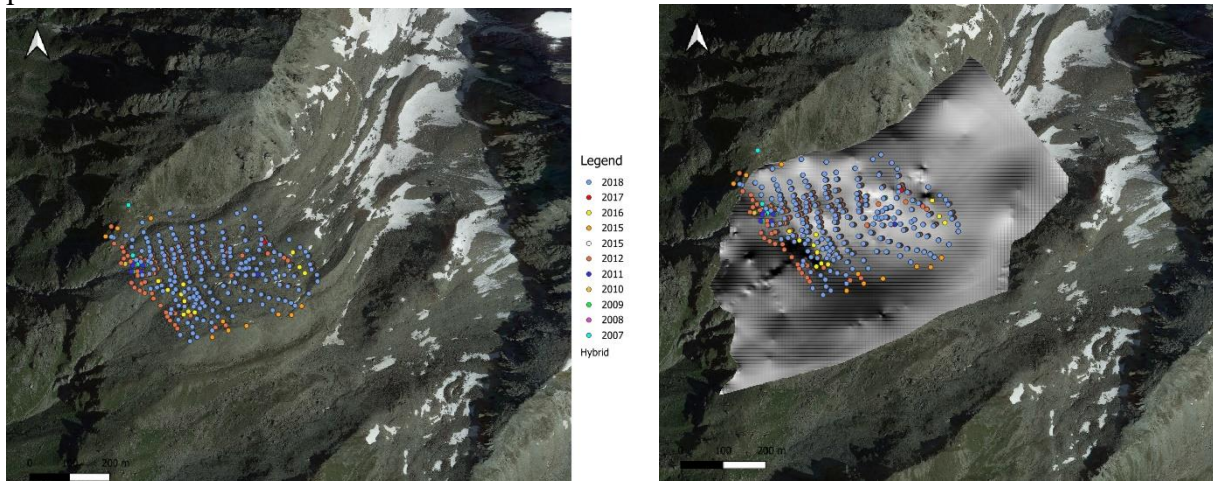


Figure 53 : Profile and plan curvature differences

#### 4.4 GPS system analysis

Situated on the studied area, GPS monitoring system was installed in 2007 and their advance has been measured until 2018; pay attention to the fact that a time jump exists between 2012 and 2015, because data for the years 2013 and 2014 are not available.

In *Figure 54*, the position of all the points is shown with and without the reference bedrock surface, in order to frame the general situation with respect to what was said in the introductory part.



*Figure 54 : GPS points in the area*

Taking advantage of *QGIS* software, it is possible to quantify what is the actual displacement of the rock glacier in this specific time span: considering the same GPS points, it results that both their coordinates on the plane X, Y changed, but also the Z one, so in the vertical direction. For the first case, it is sufficient to zoom in on the surface to appreciate the motion:

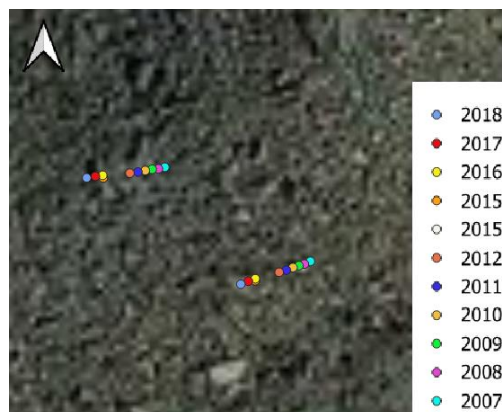


*Figure 55 : Example of GPS points' motion from 2007 to 2018*

For the example shown in *Figure 55*, a rough estimation of the distance between points from 2007 to 2018 has been measured, obtaining a value of about 11 m, which means more or less a displacement of 1 m per year on average; moreover, the temporal gap from 2012 and 2015 can be appreciated because the distance between points is bigger.

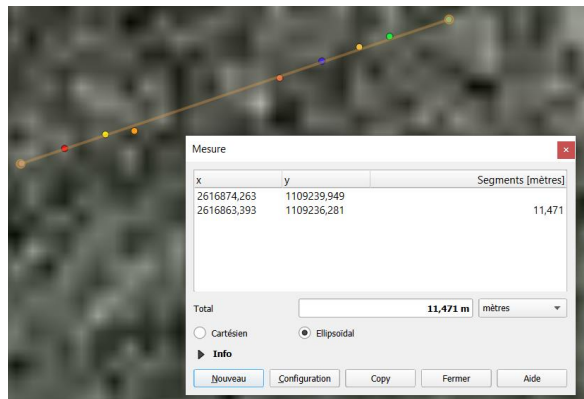


Figure 56 : Manual length measurement in QGIS

Being an ensemble of different materials, elements and typologies of rocks in terms of origin and density, motion and its direction change a lot from one point to another. Estimations for length, angle, azimuth and precisely of direction was performed taking advantage of *Fmeworkbench* software. A specific transformer calculates, in degree, the angle and azimuth of input lines by connecting two input points. Angles are measured from the reference point of East, corresponding to the 0 value and counter-clockwise positive. The azimuth is the angle between the line and the north vector (where the North coincides with 0) and again counter-clockwise positive).

Mean values of lengths unfortunately cannot be calculated because as explained, points have been added and removed through the years: for some of them the complete series of recording is available (namely from 2007 to 2018), but for some others instead not. So, making the average among different number of data will not give a meaningful result.

However, a first map was produced indicating, in an automatic graduated range from 0 to 18, the spots which have moved more or less in time: in particular, it can be noted that the majority and the most significant displacements occurred in the upper left part of the monitoring zone, the ones which results, already from the previous analysis, to be the more active.

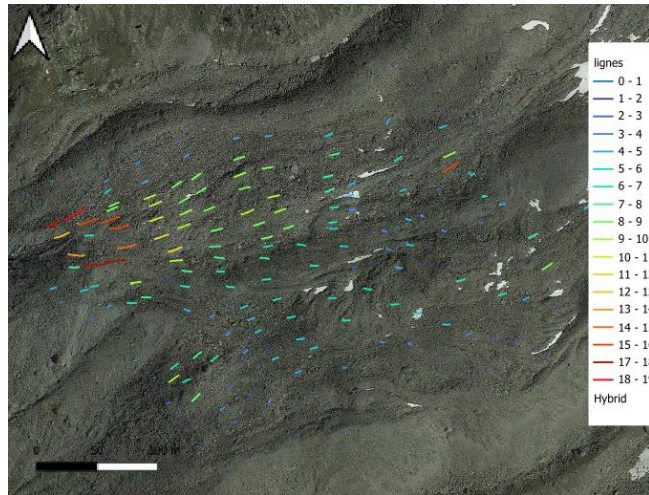


Figure 57 : Length of all displacements of rock glacier's surface material

Then, a second one allows to visually see both the flow direction and the length of motion of the GPS points thanks to the presence of arrows: in accordance with what explained while talking about the aspect, the average displacement occurred mainly towards the South-West direction.

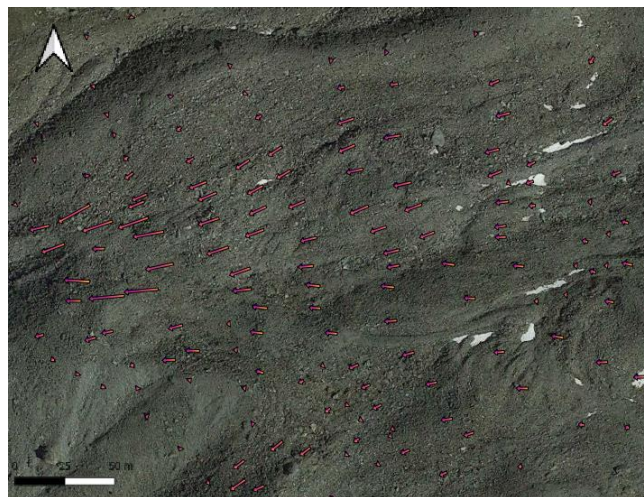


Figure 58 : Flow direction map with arrows

Furthermore, taking advantage of the Z coordinate, which indicates the elevation of each GPS station, it has been possible to calculate the variation of the mean depth of the active layer in time, over the area under analysis. Its thickness changes of several meters because the unconsolidated boulders, that predominantly composed it, move on the surface of the glacier, especially for two main reasons:

- on one side, the increment of temperature, responsible for the melting of the permafrost layer, which facilitates the sliding of the material;
- on the other side, the decrement of the snowpack height, which as seen is able to maintain all the structure more compact and to avoid rock falls or debris flows.

But in order to obtain consistent result, this kind of work has been performed only for the points for which measures have been repeated throughout all the period. So, after a filtering procedure, finally the total number of points which contribute to this estimation has been found to be equal to 80.

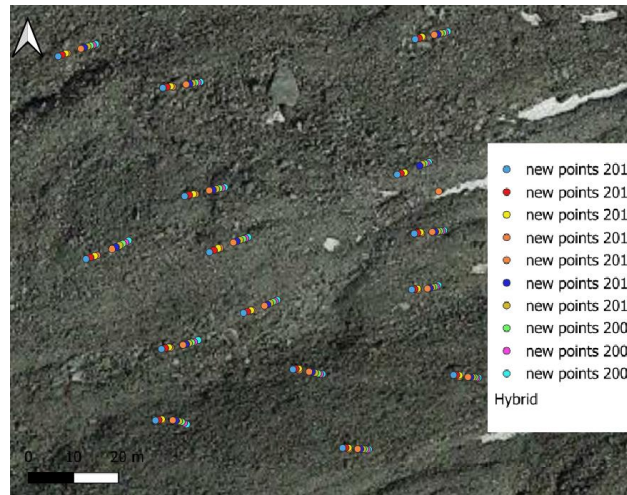


Figure 59 : Focus to see complete series of 80 points on the area of interest

Firstly, the mean elevation has been plotted and, as it can be noticed, it decreases while time passes:

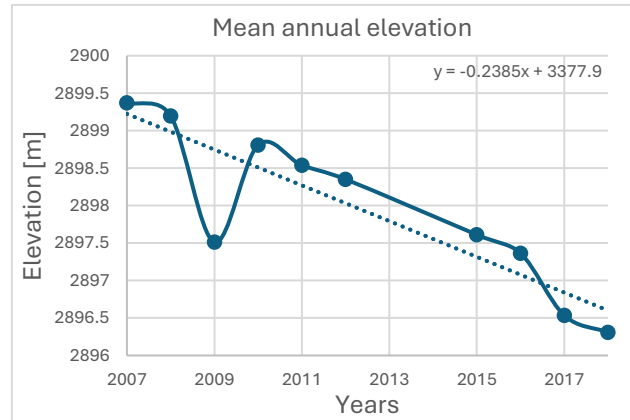


Figure 60 : 80 points mean elevation

Then, making the difference between the Z coordinate and the elevation of the bedrock's roof for each specific point, using *SAGA* software, as said, also the thickness of the active layer has been calculated for each of them; an almost linear decrement can be observed from the maximum depth in 2007 (20.3 m) to the minimum in 2018 (18.9m), with an average of 19.7 m:

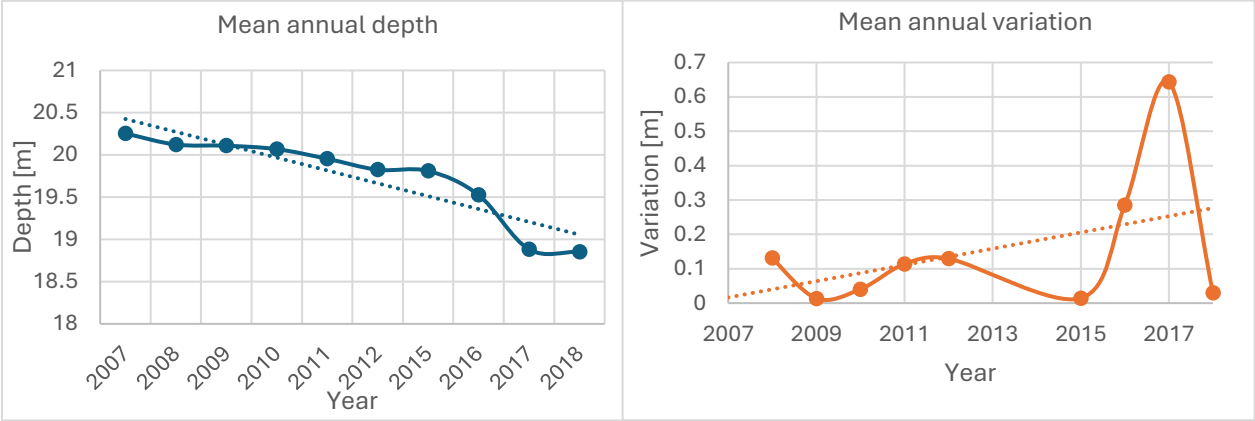


Figure 61 : Depth of material in motion with the relative variation in depth from one year to another

	<b>Mean depth [m]</b>	<b>Δ</b>
<b>2007</b>	20.25	-
<b>2008</b>	20.12	0.13
<b>2009</b>	20.11	0.01
<b>2010</b>	20.07	0.04
<b>2011</b>	19.95	0.11
<b>2012</b>	19.82	0.13
<b>2015</b>	19.81	0.01
<b>2016</b>	19.52	0.28
<b>2017</b>	18.88	0.64
<b>2018</b>	18.85	0.03

Table 4 : Annual depth and relative variations



#### 4.5 Fixed GPS

Data regarding the total movements of two GPS, installed at specific and fixed locations, in the lower part of the rock glacier, are analysed between 2010 and 2023.

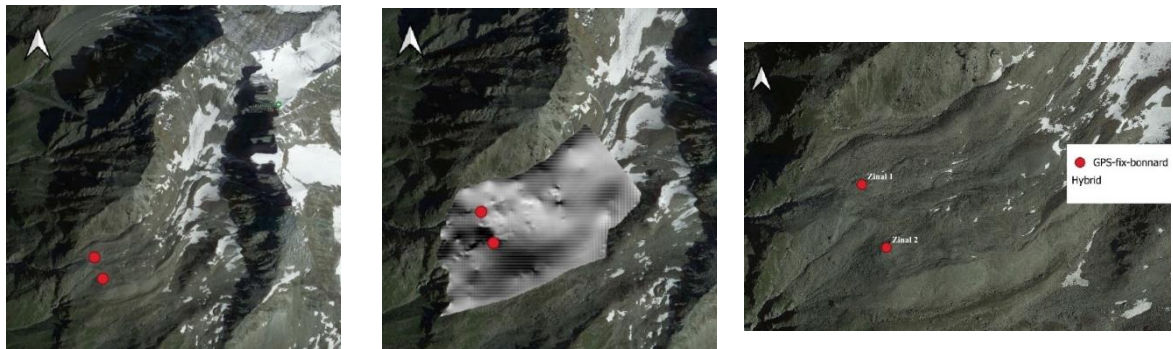


Figure 62 : Fixed GPS 's location with respect to the whole glacier and to the bedrock's roof

First of all, what it is possible to say, with respect to the surface analysis conducted above, is that the two fixed GPS are located at an altitude of about 2875 m and, respectively, GPS1, on the left side, is on a slope of about  $20^\circ$ , while GPS2 of about  $45^\circ$ ; the first, just above and the second, just below the shelf break clearly visible from the 3D view.

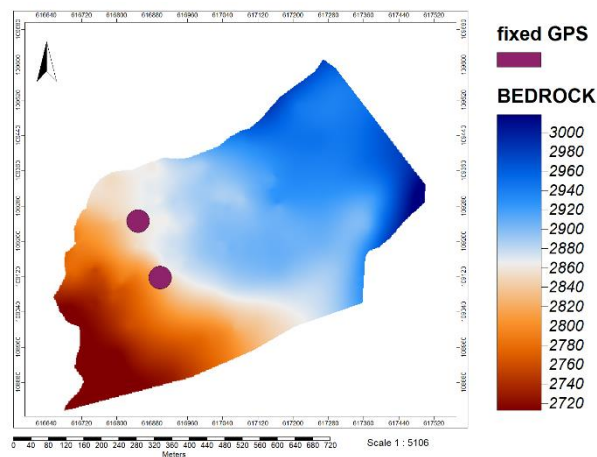


Figure 63 : Elevation of fixed GPS

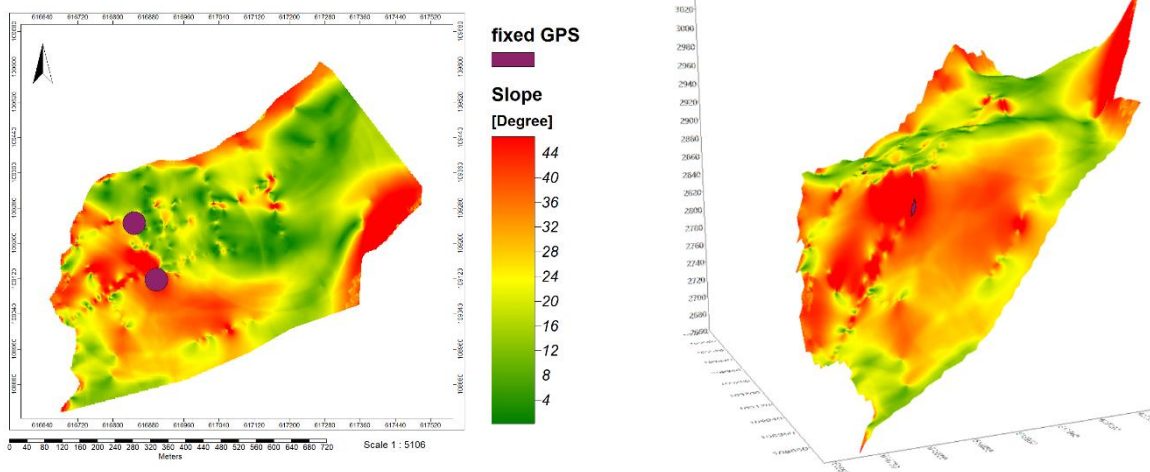


Figure 64 : Fixed GPS with respect to the slope of the bedrock's roof

Moreover, they are both installed on the part of the slope oriented towards West (about 260°), as the aspect parameter indicates.

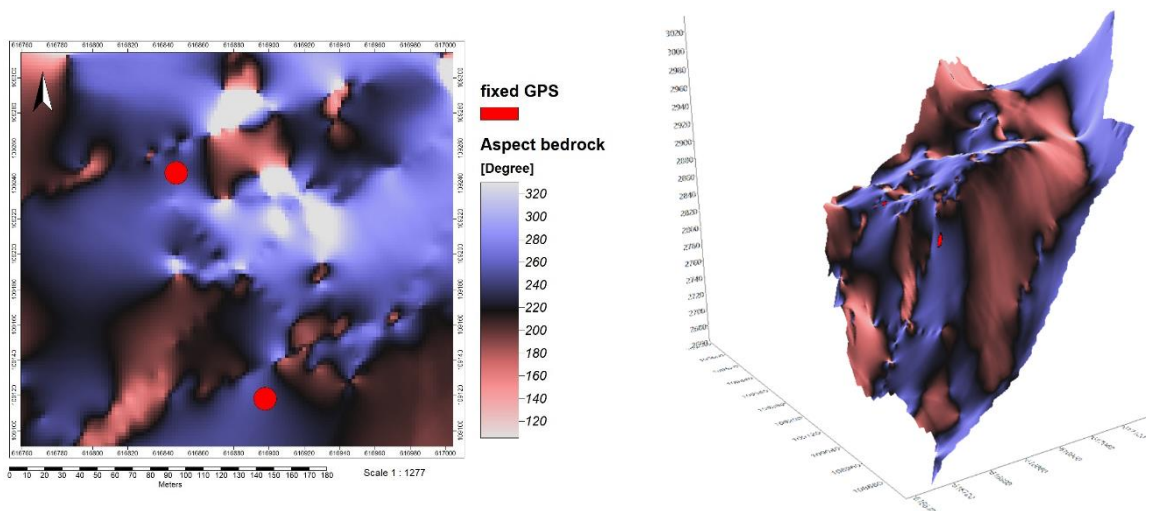


Figure 65 : Fixed GPS with respect the aspect of the bedrock's roof

In the specific, daily displacements of these points were recorded and data are provided in a cumulative way, in [m]. By simply making the difference among rows, the absolute value of daily movements can be obtained, with an average yearly displacement which is different for the two cases.

It results to be of 0.004 m for GPS1, where an increasing trend can be noted, and of 0.002 m for GPS2 (about the half), where instead the linear coefficient is negative but small, so much small that it can be considered as stable through time. This can be explained by the fact that, as known following some specific soil and matrix analyses on site, GPS1 is above a quite thick layer of permafrost, so it is subject to its thawing and freezing because very sensitive to

temperature variations, while GPS2 is not, so clearly results are at the end different, as it can be appreciated in the following graph:

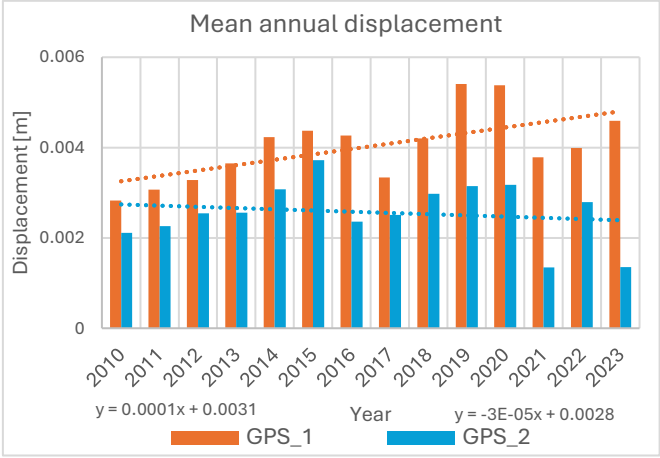


Figure 66 : Annual displacement of fixed GPS

By considering the already analysed environmental data, does a correlation can be established between the mean annual air and ground temperature at “Tracuit” station, the mean annual snowfall and the motions of the material where the GPS are placed?

For GPS1, major displacements occurred, from the biggest to the smallest, in 2019, 2020, 2023, 2015, 2016, 2014 and 2018 (values major than 0.004 m/year) concurrently with the highest recorded air temperature (more than 1°C). These are the cause of more heat transferred to the upper layers, namely the ones in contact with the troposphere, phenomenon which triggers and amplifies the snow melting (during the periods of the year when it is present) with the consequent flow and infiltration of water in the surface’s material: all these elements contribute to increasing the instability of the area.

Ground temperature, instead, have not been considered because, as seen, they don’t vary a lot through the considered years: evidently the conductive process which governs the heat transfer is not so effective due to the fact that the thickness of the overall structure is of several metres. The external warming is, for the moment, neither reaching nor influencing the glacier’s bedrock characteristics and stability in a significant way.

Looking at the precipitation side, lower snowfalls were recorded, specifically in 2010, 2011, 2015 and 2022, but they seem not to impact directly the motion of the material.

For GPS2, instead, it is more difficult to try to create a link among factors: the only statement is that it moves less than GPS1 through time.

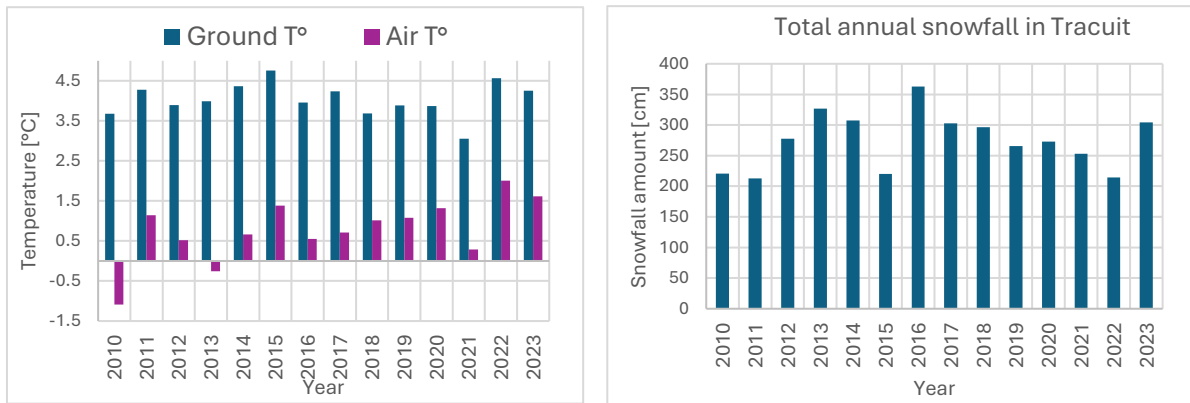


Figure 67 : Environmental data at "Tracuit" station from 2010 and 2023

Clearly, the studied phenomenon is very complex, lots of parameters influence it and moreover the response of the system is not immediate.

If temperature increase exponentially within a short time frame, the effects are surely more evident with respect to the case in which, instead, temperature raise but in a less abrupt way: in this last case, for instance, the consequences can surely be seen, but in another period and/or when particular conditions occurred. In addition, these considerations are made on averages during years in which the alternation of the seasons change completely the situations. For that, in order to try to be a little bit more precise, the analysis continues by focusing on winter and on summer variations through the different years.

In order to analyse the results, it has been decided to consider January, February and March inside the class of winter months, while July, August and September for the summer ones (not June because at such altitude snow is still present and so results would be biased).

To better explain the process, it is useful to look at temperature and precipitation data both in winter and in summer and to consider their trends through those years, to establish, as already mentioned, a correlation between the events.

Winter months are characterised by negative air temperature which show a significant increase, especially during the last four years. Values are always much smaller than 0°C and in fact, on average, only solid precipitation are recorded in that area, as shown in the following pie chart.

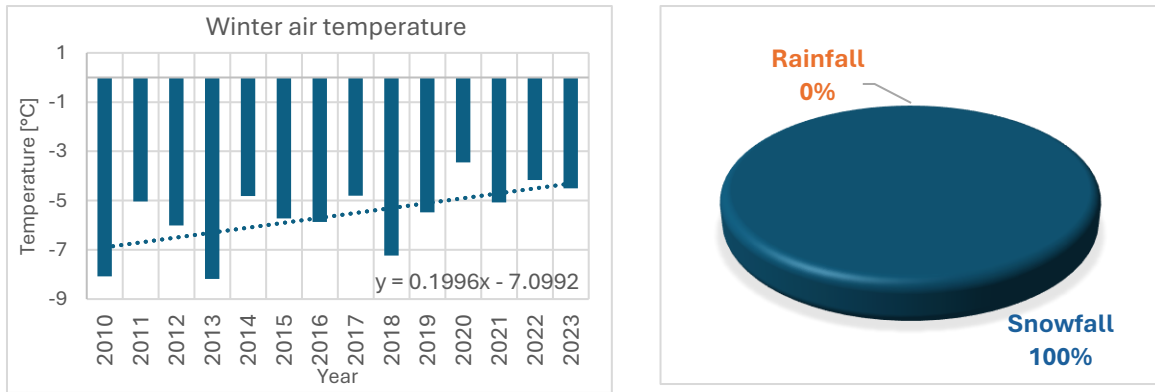


Figure 68 : Mean winter air temperature and typology of recorded precipitation

Considering instead the mean trend of precipitation, this results to be negative, meaning a decrement of snowfall in the period under analysis; moreover, coherently with the raise of temperature and the decrement of solid precipitation, it happens that the snowpack height is in evident reduction. This is an important cause of instability of the surface material because in winter, snow becomes ice, element which is capable to increase the strength and the cohesion among materials, acting as cemented element. Anyway, until now, in all its forms, the total amount of snow is declining, but fortunately, at least during winter months, it is not extremely low, near alarming zero levels: this means that the effects are not so visible yet, starting to appear, rapidly getting worse if the explained trends will proceed in the same direction or in an intensified one. Having generally said that, it is now time to focus separately on the two available sets of data.

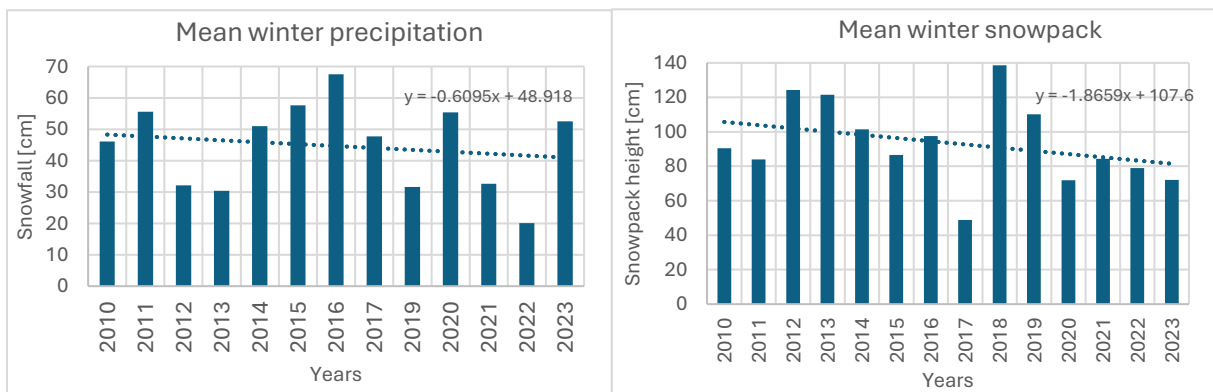


Figure 69 : Mean winter precipitation and snowpack at "Tracuit" station

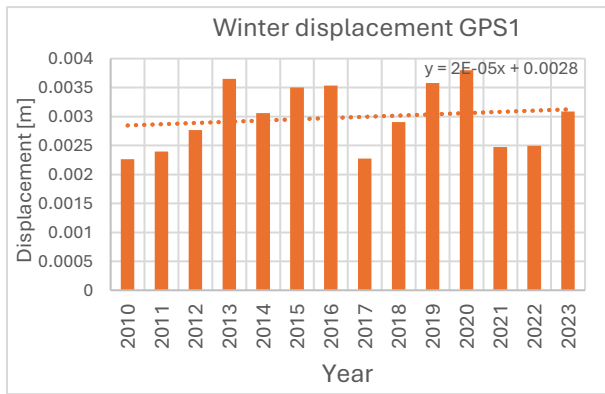


Figure 70 : Mean winter displacement of GPS1

Starting from GPS1, the trend of motion is positive even if it is not so extremely marked; in line with what just explained, throughout all the years under analysis, mean values of temperature result to be below 0°C, indicating the presence of frozen water (ice) in rock glacier's matrix which implies a considerable stability.

Air temperatures are increasing with a clear positive trend of about 0.2 °C between 2010 and 2023, but this growth seems only beginning to affect the stability of the material in this specific zone, during the colder months of the years.

The minor recorded value of displacement is 0.0022 m in 2010, while the major is 0.0038 m in 2020, with a mean of 0.0029 m in 13 years and a increment of 0.0016 m: temperature in 2010 is one of the lower (-8.1°C), in 2020 is the higher (-3.4°C) and so it seems that a correlation can be established between these two parameters due to the fact that the major displacement happens concurrently with the major temperature.

But looking at the plot, the biggest displacements (all greater than 0.003 m per year) occur also in 2013, 2015, 2016, 2019, 2020: in this case, a direct link between temperature and movements seems not to exist. Actually, as said, the effect of temperature can be more impactful if their raise is very high otherwise their effect can be delayed in time, during other seasons of the year. Moreover, as mentioned in the previous chapters, temperature is only one of the main factors driving rock glacier's deformation: in fact, precipitation amounts need to be considered, because more or less amount of snow differently affects the stability overall. In fact, in 2013 and 2019, with respect to the mean, very low snowfall occurred, while in 2015 and 2016 greater amounts were recorded, but with minor accumulation on the surface, as found by snowpack height.

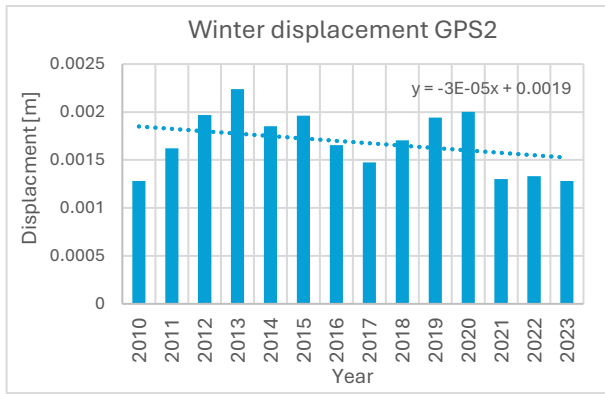


Figure 71 : Mean winter displacement of GPS2

For GPS2, instead, the trend is negative, but also in this case quite negligible and displacement's values are about one order of magnitude lower than for GPS1, with a minimum value of 0.0012 m in 2023 and a maximum one of 0.0022 m in 2013 with a mean of 0.0017 and a variation of 0.0010 m. The fact that the peak of the displacement is in 2013 and not more recently (like 2020 for

the first case) and that values are not increasing, is because this GPS is in a stable zone, where the material is mainly composed by rocks, boulders and debris without or with few amounts of interstitial ice, so more independent from weather factors. In addition, with cold temperature, as mentioned, all the structure remains more compact.

Saying that, for what it has been explained at the beginning of this section, the increment of mean displacement is evident in the case of GPS1 and so the only possibility is that this happens during other periods through the year, like during hottest months: in fact, a completely different scenario comes if summer periods are considered. They are characterized, as a matter of fact, by a significant increment of temperature and a consequent significant decrement of the snowpack height, together with a decrement of precipitation (which result to be only liquid due to the fact that 0°C level is never reached).

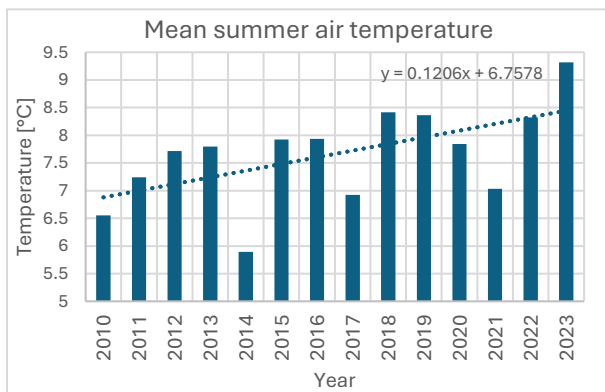
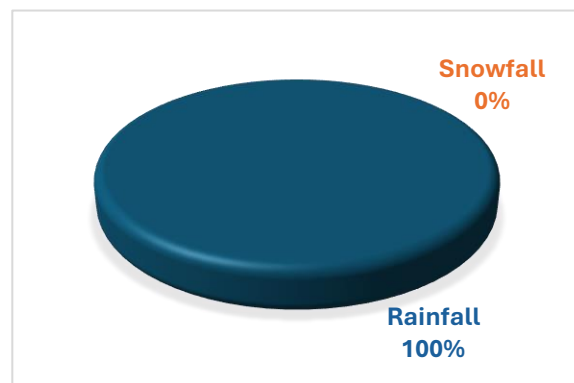


Figure 72 : Mean summer air temperature and typology of recorded precipitation



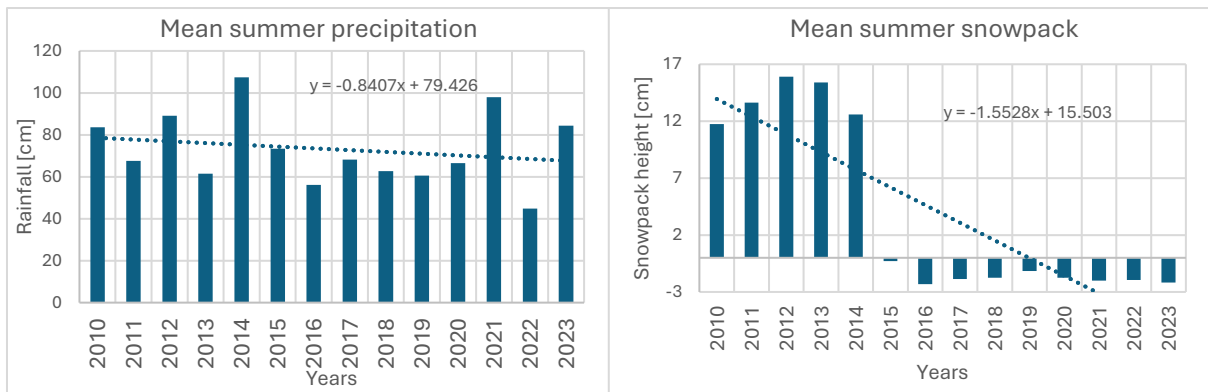


Figure 73 : Mean winter precipitation and snowpack at Tracuit station

In this case, for both data, trends of movements are positive meaning that inevitably high temperature have a concrete and direct impact on the main deformations occurring at the surface, because their raise is significant. In the specific, if under GPS1 is the layer of permafrost which is melting and so it is mainly responsible of its motion, GPS2 can be considered more stable, with movements which can be associated to water percolation coming from other upstream areas, or due to extreme precipitation events, which are less frequent (which is an explanation of the fact that the total amount of precipitation is decreasing), but more intense and so impactful. When such events occur, water has no time to infiltrate and so it increases the runoff phenomenon, which can be another cause of boulders' motion and also the cause of the formation of mud and its flow.

Specifically:

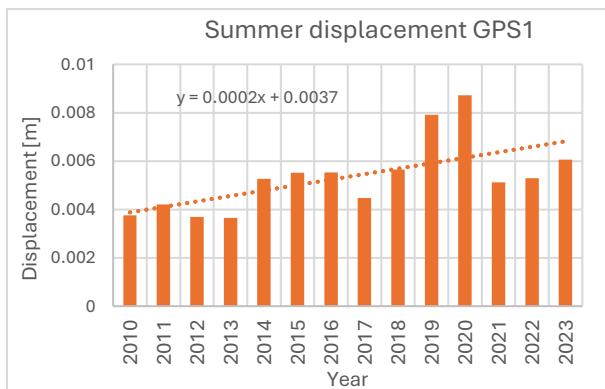


Figure 74 : Mean summer displacement of GPS1

for GPS1, displacement's values range from 0.0036 m to 0.0087 m with a mean of 0.0053 m and peaks in 2019 and 2020. Moreover, the trend is one order of magnitude bigger than winter's one (+ 83% by looking at the mean displacement), because temperatures are greater (in mean 12°C higher). This reflects on the behaviour

of this part of the glacier which, therefore, results to be in acceleration in these 13 years.



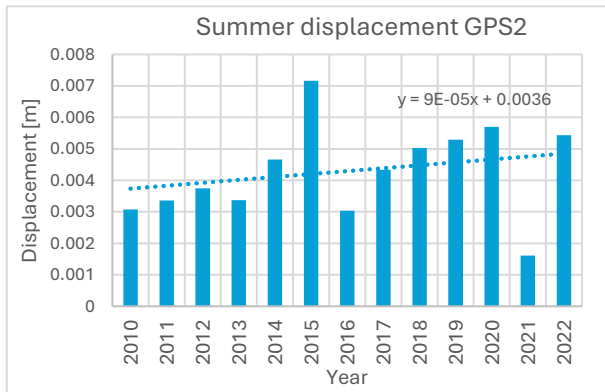


Figure 75 : Mean summer displacement of GPS2

For summer months, GPS2 data are available until 2022. Displacement's values are lower with respect to the previous case, ranging from 0.0016 m to 0.0071 m with a mean of 0.0043 m, which is 23% less than GPS1 movements. With respect to the winter case, instead, the increment is of about 150%, underlying once again the great

impact of climate warming on the periglacial environment.

Now, in order to better visualize these results, graphs with the comparisons between winter and summer are shown in the following, for both instruments:

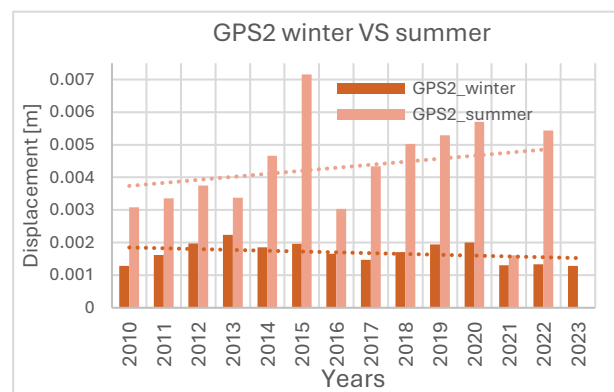
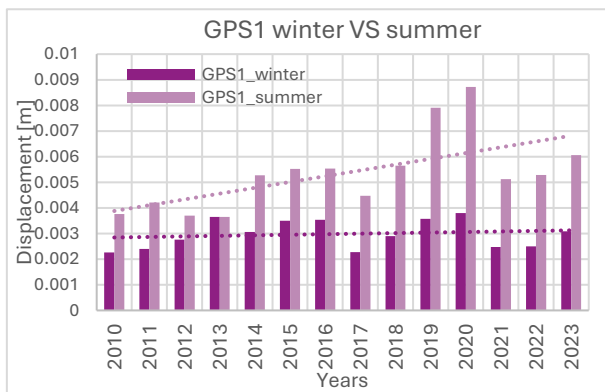


Figure 76 : Mean displacements in winter and in summer

It can be appreciated a huge difference between winter and summer, as expected, but also between years, with displacements ranging from more than 0.002 m to nearly 0.004 m for GPS1 and from 0.001 m to 0.002 for GPS2 during winter months and between 0.004 m and 0.009 m and 0.002 m and 0.007 m respectively during summer, basically indicating almost a doubling of the acceleration of rocks and debris.

## 4.6 Velocity's analysis

But which are the areas that move more and where are they located with respect to the entire rock glacier? How does the speed of motion changes during the years?

Answers come from GPS data: from their coordinates, velocities of the 80 points, for which all records are available, as explained, can be calculated from one year to the other, as the ratio between distances of the three coordinates and time. Then, the 3D velocity, again for each point, is obtained through the formula:

$$V = \sqrt{v_x^2 + v_y^2 + v_z^2},$$

which is applied separately for the negative and the positive values, indicating respectively deceleration and acceleration. Then, the average between these two results is performed and, at the end, the mean final speed of the surface values is obtained; as it can be appreciated in the following plot, it shows a positive trend.

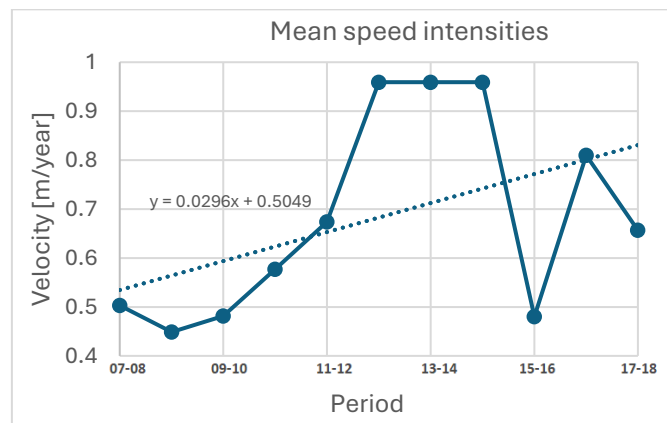


Figure 77 : Mean velocity of the area coinciding to the bedrock's roof

Actually, the peak joined in 2015 is followed by a decrement which can be explained, in part, by the huge amount of snow fallen especially during the winter of 2016, which was recorded higher than the mean over the period. In addition, this together with lower air temperature recorded during 2017 and especially during the summer period, fact which helped the snowpack to remain more at soil and to give stability to the area.

### 4.6.1 General velocity's maps overview

Then, based on the available GPS measurements, so georeferenced with their own coordinates, series of maps (available from 2007 to 2017) representing velocities' variations between two years were created by Eric Bardou and his team and dates available for this study; this using *Isatis*, a specific software designed for the use of geostatistics, which from data, produces high-quality maps and models.

Due to the fact that a degraded network is the result of the available GPS points, maps were obtained by resorting to the collocated cokriging technique, to rely on other information available at higher density and well correlated to the target variable, to reduce overall the uncertainties in the results (E. Bardou G. F.-B., 2015).

In general, stable parts are more visible on the edges, while the central part is the one which moves more and it is in acceleration with the two lobes which characterize the rock glacier which are clearly visible. The principal hotspot remains always the one already pointed out from GPS system results, located in the lower left part and coloured in red. Moreover, the general speed is increasing overall the considered surface, as the scaled bars and the maximum reached values indicate.

	<b>Max speed [m/year]</b>
<b>2007-2008</b>	0.86
<b>2008-2009</b>	0.78
<b>2009-2010</b>	0.89
<b>2010-2011</b>	1.09
<b>2011-2012</b>	0.95
<b>2012-2015</b>	4.02
<b>2015-2016</b>	0.73
<b>2016-2017</b>	1.18

Table 5 : Maximum speed joined on the surface, from maps created with Isatis

Specifically, detailed results are listed below.

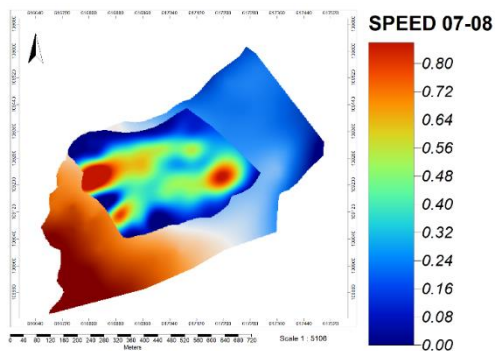


Figure 78 : Speed map 2007-2008

The first period in analysis is taken as a reference one, to compare what happened then in the following years. Together with the already mentioned hotspot, also another one is visible, at higher elevation, on the right part of the layer. These two are the points where materials are more subject to acceleration and speed's value are the highest (around 0.80-0.86 m/year).

From now on, to be clearer and more synthetic, from left to right, the two areas are renamed as SPOT1 and SPOT2.

<b>2007-2008</b>	<b>Max value [m/year]</b>	<b>Mean value [m/year]</b>
	0.86	0.50

Table 6 : Summary 2007-2008

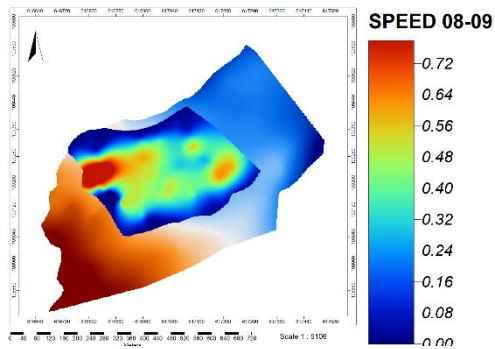


Figure 79 : Speed map 2008-2009

The year after, the situation can be considered very similar and quite stable. SPOT1 moves more or less at the same rate (0.78 m/year), while SPOT2 is a bit decelerating passing to a velocity of 0.65-0.70 m/year.

2008-2009	Max value [m/year]	Mean value [m/year]
	0.78	0.45

Table 7 : Summary 2008-2009

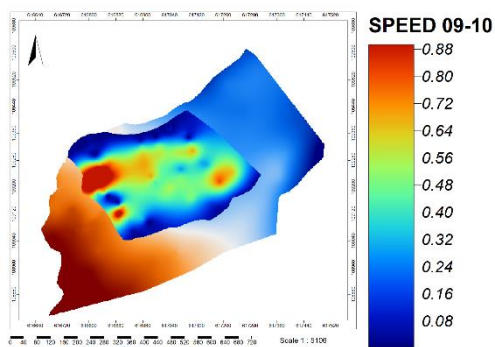


Figure 80 : Speed map 2009-2010

The third period is characterized again by a small increment which also concerns in a clearer way also the second lobe, so the lower central part on the map.

2009-2010	Max value [m/year]	Mean value [m/year]
	0.89	0.48

Table 8 : Summary for 2009-2010

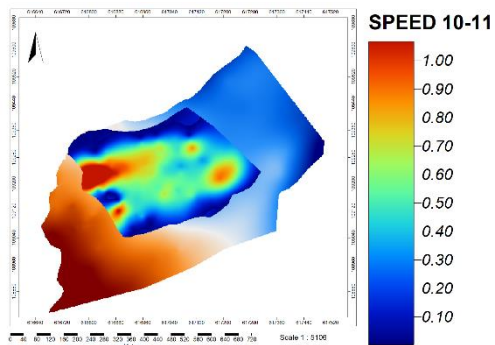


Figure 81 : Speed map 2010-2011

Together with higher temperature and lower solid precipitation, inevitably surface's speed increases overall, with SPOT1 which reaches one of the major values: 1.09 m/year.

2010-2011	Max value [m/year]	Mean value [m/year]
	1.09	0.58

Table 9 : Summary for 2010-2011

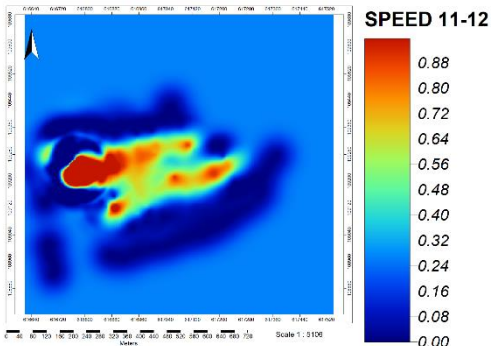


Figure 82 : Speed map 2011-2012

Unfortunately, this map had some problems during the visualization. Anyway, this error allows to better highlight the acceleration of all the material standing in the middle and to clearly see the two lobes above mentioned. The speed, from now on, starts increasing following temperature rising.

2011-2012	Max value [m/year]	Mean value [m/year]
	0.95	0.67

Table 10 : Summary 2011-2012

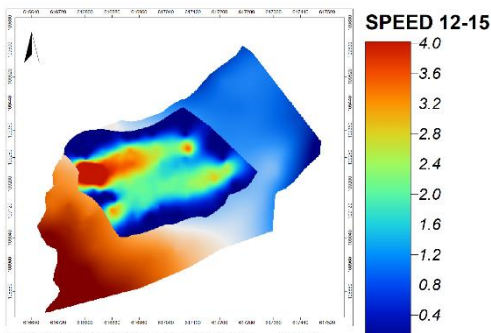


Figure 83 : Speed map 2012-2015

This map includes three years of motion because speed's differences were calculated between 2015 and 2012 directly.

Assuming that during this longer period the displacements remain stable, even if previous results prove that is not exactly like this, a rough estimation allows to conclude that on average the speed has been of 0.72 m/year. Again, SPOT1 is the one which

accelerates mostly, with a mean of 1.34 m/year.

2012-2015	Max value [m/year]	Mean value [m/year]
	4.02	2.16

Table 11 : Summary 2012-2015

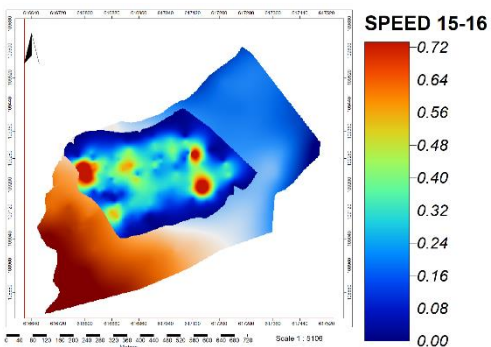


Figure 84 : Speed map 2015-2016

With respect to the previous years, an overall deceleration can be noticed. Even if it is less important for SPOT1, the central part instead appears to be more stable. This is completely in accordance with the mean velocities calculated and plotted in the section before that one.

2015-2016	Max value [m/year]	Mean value [m/year]
	0.73	0.48

Table 12 : Summary 2015-2016

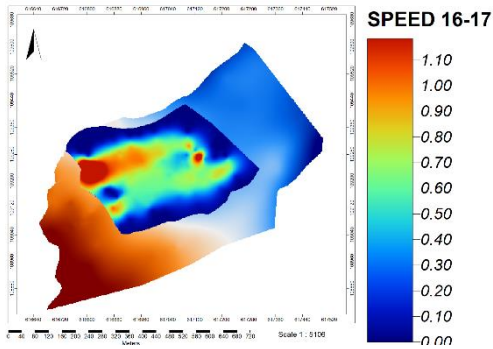


Figure 85 Speed map 2016-2017

Finally, again, during the last analysed years, the acceleration becomes one more time very evident, with the part in the middle showing values from 0.60 to 1.18 m/years and this is completely in accordance with what was obtained through the calculus.

2016-2017	Max value [m/year]	Mean value [m/year]
	1.18	0.81

Table 13 : Summary 2016-2017

After that, coherently with the analysis implemented by taking advantage of the aerial photogrammetry tools, differences among grids of specific years are calculated through *SAGA* software. In Chapter 3, surface's variations and boulders' motion were considered between:

- the longest available period, namely 13 years, between 2007 and 2020. In reality, speed data are recorded until 2017, so this comparison is reduced to 10 years;
- then, between 2010 and 2016, in order to consider the central period and approximately half of the time previously analysed;
- finally, the difference between the first two years (2007-2009) and the last two years (2015-2017) of monitoring, to see if an evident acceleration can be noticed more recently.

#### 4.6.2 Years from 2007 to 2017

It is evident that over the entire period, mainly the central part of the glacier is the fastest, in accordance with all the previous results; whereas on the sides, the material is almost stable or little decelerating, because the frictional force is higher.

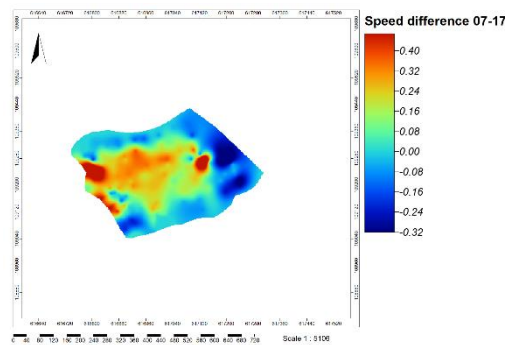
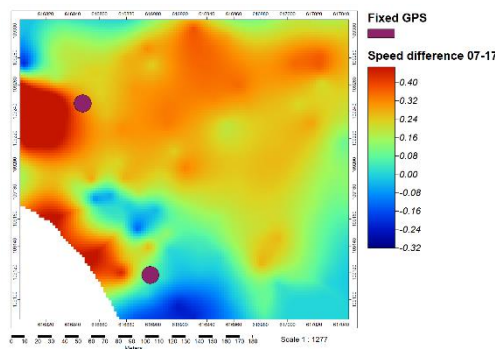


Figure 86 : Speed difference map calculated between 2007 and 2017

Moreover, over this time frame of 10 years the maximum increment of speed has been of 0.47 m in correspondence to the red parts, namely of the already known SPOT1 and SPOT2, with the majority of the area which results to accelerate. Little decrement can be seen instead at the higher elevations.

In addition, completely in accordance with the displacements recorded for the two fixed GPS, GPS1 is in the orange-red area, the one with higher speed, while GP2 is in the aqua-green colour, the more stable instead, as it can be appreciated from the zoom in *Figure 87*.



*Figure 87 : Zoom on fixed GPS with respect to speed intensity variation between 2007 and 2017*

To explain this evident phenomenon of acceleration, again, it is necessary to resort to temperature and snow data, considering the mean parameters both for 2007 and for 2017, separately, in order to compare them in the proper way. In particular, what is in the column of 2007 is the mean between values of 2007 and 2008 to be in accordance with the speed map which record the variations from one year to another; the same for 2017 which is the result of averages between 2016 and 2017.

	<b>2007</b>	<b>2017</b>	<b><math>\Delta</math></b>
<b>Air temperature [°C]</b>	+ 0.1	+ 0.6	+ 0.5
<b>Ground temperature [°C]</b>	+ 3.9	+ 4.1	+ 0.2
<b>Snowpack height [cm]</b>	46	33	- 13
<b>Snowfall precipitation [cm]</b>	318	332	+ 14

*Table 14 : Environmental data for years 2007-2008 and 2016-2017*

Whether they are increment or decrement, variations are significant, with an evident impact on the amplification of the speed intensities through time. Specifically:

- an important rise of air temperature, more than the ground one for the reasons already explained in the other sections, which contributes to the permafrost melting;
- a decrement of the average snowpack height, which decreases the cohesion of the material and so structure's stability;

- a small increment of snowfall, linked to the already cited anomaly of 2016, with lower temperature and higher precipitation with respect to mean values, with repercussion on the following years (namely 2017 and 2018, as known from data).

#### 4.6.3 Period from 2010 to 2016

Considering more or less the half of the years, that is six, instead, all the structure appears to be more stable, with lower significant velocities' variations which can be appreciated: looking at *Figure 88*, the motion of the surface material immediately results to be generally minor with respect to the previous case and this can be partly explained by the environmental data.

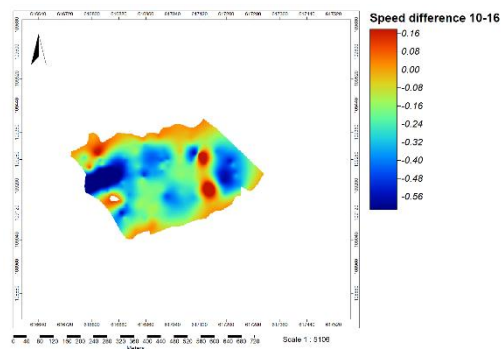


*Figure 88: Speed difference map calculated between 2010 and 2016*

Again, for 2010, values are the mean between 2010 and 2011, while for 2016, the mean is between 2015 and 2016.

With respect to the previous case, air temperature increment is higher, but this element is compensated by the concurrent huge rise of snowfall over the period:

	<b>2010</b>	<b>2016</b>	<b><math>\Delta</math></b>
<b>Air temperature [°C]</b>	+ 0.03	+ 0.9	+ 0.9
<b>Ground temperature [°C]</b>	+ 3.9	+ 4.3	+ 0.4
<b>Snowpack height [cm]</b>	44	39	- 5
<b>Snowfall precipitation [cm]</b>	216	290	+ 74

*Table 15: Environmental data for years 2010-2011 and 2015-2016*

As final result, surface's deformation is minor and the parts that on the average long period are in movement, here they are not (stable or almost decelerating).



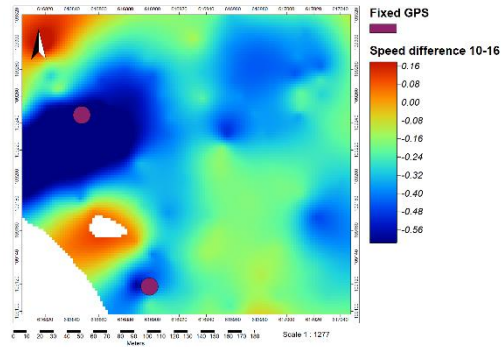


Figure 88 : Zoom on fixed GPS with respect to speed intensity variation between 2010 and 2016

Interesting to notice that, in correspondence with SPOT1, where GPS1 is located, an important deceleration is evident: this can be explained by the presence of more snow during winter months which brings more cohesion to the materials.

From this analysis, it can be affirmed that all the displacements are heterogeneous both in time and in space: mean trends say that overall, an acceleration is occurring, but not linearly through years, with some variations due to the complexity of the system.

#### 4.6.4 Short period: two years

Considering the final studied case, the results confirm all what it has been said until now, also in the above Chapters: today more than in the past, material on the surface is moving downslope with an important increment of the speed: if its variations were low, at the beginning of the monitoring, instead at the end, the acceleration, especially of the central part, is very evident.

It can be noted that, over the first short amount of time, on average, all the area can be assumed to be stable, with little decrement of velocity near SPOT2 and very little increments visible just above.

The maximum variation in the speed intensity is, in fact, of 0.16 m in two years, meaning 0.08 m/year.

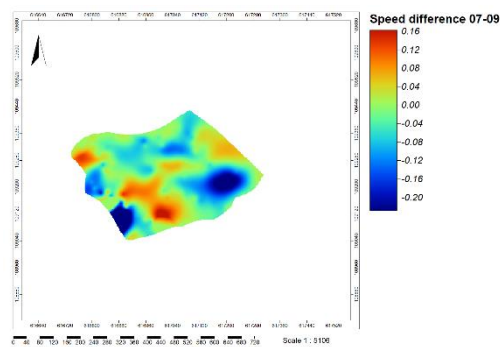


Figure 89 : Speed difference map calculated between 2007 and 2009

In the second period instead, the maximum variation is of 0.65 m, that is around 0.33 m/year, 0.25 m more than the previous case: this acceleration of the material downstream is highly visible in correspondence of SPOT1, with an evident increment of speed of all the central area.

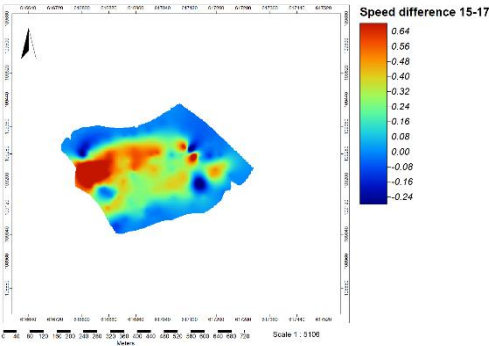


Figure 90 : Speed difference map calculated between 2015 and 2017

The environmental data confirm this trend. Making the averages from 2007 to 2009 and from 2015 to 2017, it follows that:

	<b>2007-2009</b>	<b>2015-2017</b>	<b>Δ%</b>
<b>Air temperature [°C]</b>	+ 0.3	+ 0.9	+ 0.6
<b>Ground temperature [°C]</b>	+ 4.1	+ 4.8	+ 0.7
<b>Snowfall precipitation [cm]</b>	339	295	- 44
<b>Snowpack height [cm]</b>	49	44	- 5

Table 16 : Environmental data for years 2007-2009 and 2015-2017

- air temperature’s increment is evident and this is linked to the major rate of movements of the surface’s material;
- ground temperature, instead, grow but always less rapidly;
- the decrement of snowfall is recently more important with lower and lower recorded values which relate to lower accumulation on soil, alarming in term of slope stability, as known.

## 5. Chapter 5: Final comparison

It is time to move towards a comparison between the orthophotos from the aerial photogrammetry and the speed maps, in order to try, at a later time, to find out information related to the possible amount of material which could move downslope, endangering Zinal village located just below.

To address the first point, two specific variations have been considered: 2009-2010 and 2016-2017. This to be able to compare photos and maps in the same years on one side and to highlight differences between the beginning and the end of the monitoring activities.

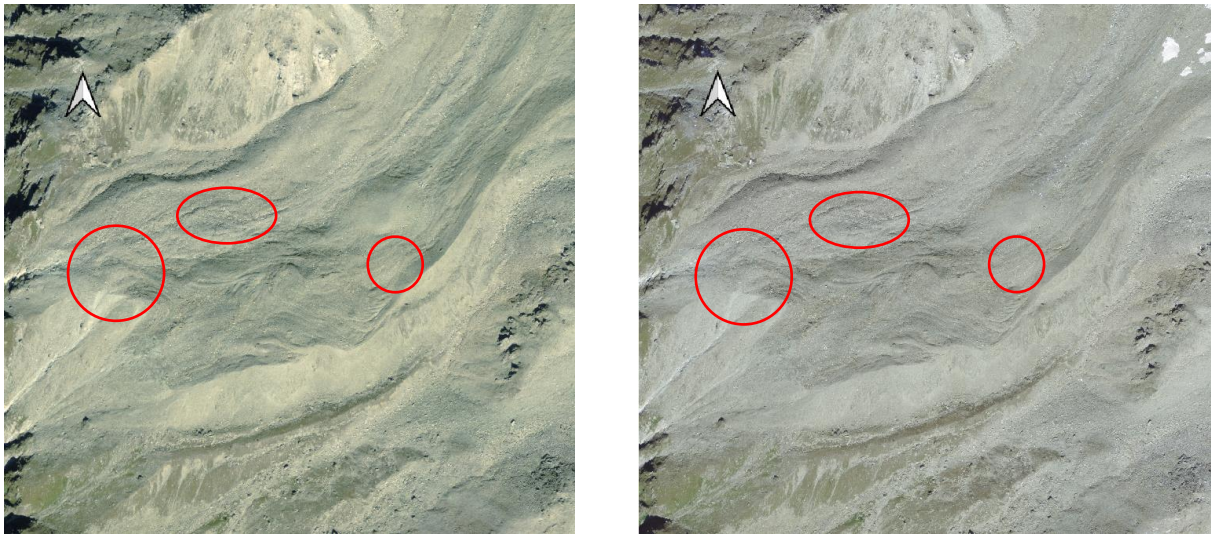


*Figure 91 : Orthophotos of 2009 (left) and 2010 (right) with the moving areas*

In the first considered period, the area which moves more is in correspondence with the advancing lobe 1 where on its turn SPOT1 is located: the three major displacements can be detected from images and are exactly the same indicated by the speed map and circled in red.

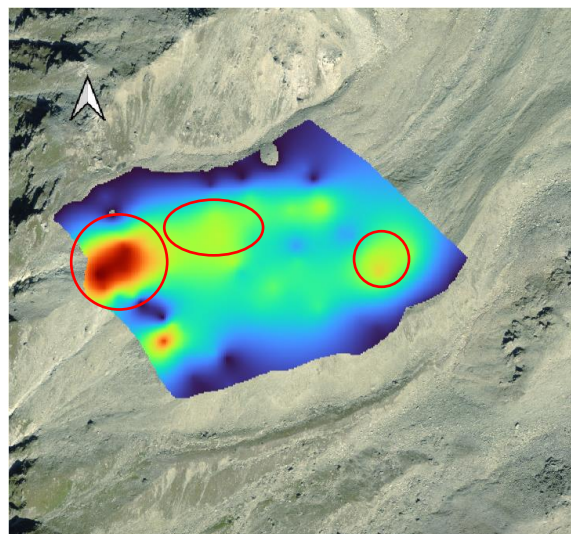


*Figure 92 : Speed map 2009-2010 on the corresponding orthophoto*

In the second period, it is obtained that:



*Figure 93 : Orthophotos of 2016 (left) and 2017 (right)*

From 2016 to 2017, there have been huge displacements on the surface with a mean speed of 0.89 m against 0.48 m measured from 2009 to 2010, so nearly the double, as explained in the previous section. And they are clearly visible also from the images. Once more, even by naked eye, it can be said that lobe 1 is the one which moves more, exactly in accordance with what the speed map highlights:

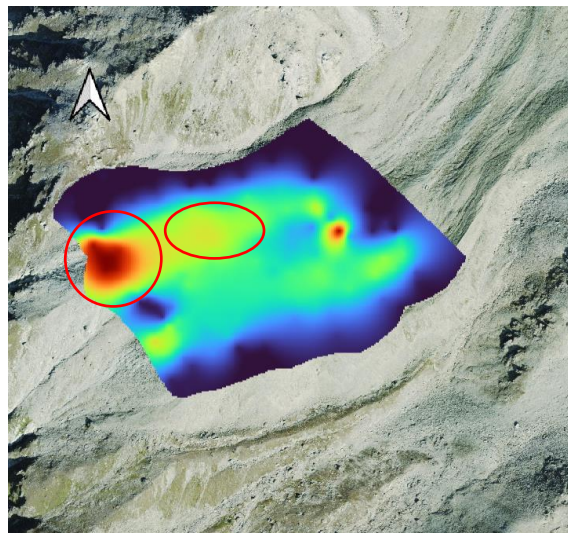


*Figure 94 : Speed map 2016-2017 on the corresponding orthophoto*

For the second point, instead, lobe 1 is considered as the most dangerous area for the considerations previously made: it is the one which accelerates mostly and moreover it is exactly the source of Pétérey torrent, the most affected by lava streams. Taking advantage of *QGIS* software, an estimation of the possible unstable volume is calculated: by considering on one side the orthophoto of 2017 and on the other the speed map of 2016-2017, (which are the

more recent available) the approximate area (A) is obtained by simply using the “measure area” tool, which allows to create a polygon around the zone of interest.

Two calculations are performed considering:

- only the strict area near SPOT1 (so the red one in *Figure 95*), which results to be around 8 600 m<sup>2</sup>;

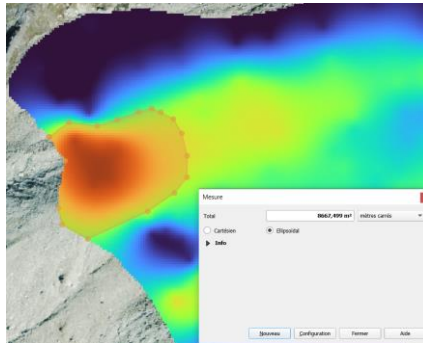


*Figure 95 : Area measurement with QGIS around SPOT1*

- all the lobe 1, which is around 14 600 m<sup>2</sup>;

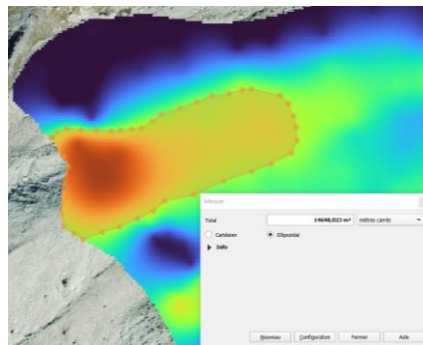


*Figure 96 : Area measurement with QGIS of lobe 1*

knowing the mean depth (h) of the active layer for the same year, which is of 18.85 m, from Chapter 4.4, having considered the volume the one of a parallelepiped, the approximative volume is calculated as follows:

$$V = A \cdot h.$$

For the first case,  $V_1 = 8\,600 \cdot 18.85 = 162\,110 \text{ m}^3$ , while for the second  $V_2 = 14\,600 \cdot 18.85 = 275\,210 \text{ m}^3$ .

Actually, the result can be considered as a rough estimation of the total volume of the material which is in acceleration over the slope, but not necessarily all of it will contribute to an imminent lava stream. Moreover, the calculated value is very high and disproportionate with respect to the figures supplied when mentioning it in the introductory part.

A more precise estimation, instead, can be carried out taking into account the fact that the rate of sediment which can reach the foot of the rock glacier depends on mainly four factors: (R. Lugon, 2010)

- mass-transfer rates produced by the rock glacier creeping;
- volume of ice and voids in the moving rock glacier section;
- rate of non-consolidated material accumulations due to active layer failures triggered by debris flows;
- permafrost ice lenses exposed at the surface.

These aspects are summarized in the following formula, which gives as result the volume  $V$ :

$$V = \frac{1}{2} * (v * W * D) = \frac{1}{2} * (118 * 70 * 15) \sim 62\,000 \text{ m}^3,$$

with  $v$ , the creep velocity [ $\text{cm year}^{-1}$ ],  $W$ , the width of the interested area [m] and  $D$ , the depth of the shear zone [m].

The calculated value is not so far from the predicted volume of more or less 40 000  $\text{m}^3$  of dangerous material looming over Zinal which can derived from Pétérey torrent: the resulting discrepancy is mainly due to the presence of voids and ice in the rock glacier body, which needs to be taken into account, adding also the fact that when the ice melts, the deriving water occupy a lower total volume. This amount is different for each glacier because clearly dependent on its composition, sediment production rate, morphological characteristics: for Bonnard glacier, this factor is estimated to be around 1.55.

Finally, it is clear that the order of magnitude of the potential unstable material is significant and for that, due to the fact that the environmental trends are unfortunately now well delineated, the only possibility turns out to be the implementation of more mitigation and adaptation actions, in order to be able to protect the village together with the ski areas.

## 6. Chapter 6: Mitigation and adaptation strategies

In this short paragraph, some possible actions are so discussed.

First of all, in order to be constantly aware of the situation and of the new evolutions, monitoring activities, which, as said, stopped in 2018, should restart to understand the entity of the recent deformations. Not only with GPS system, but also with other geophysical techniques which are already in use for the analysis of other rock glaciers: both ground-based approaches both air and space borne ones are brilliant solution for an high resolution monitoring (A. Kääb V. K., 2003).

For instance, the use of the terrestrial laser scanning (TLS) which is renowned for the fact that it is a very solid monitoring technology, so perfect for the rock glaciers. (N. Shen, 2023) Moreover, it is very accurate in capturing the spatial coordinates of target objects (sub-millimeter-level precision is also achieved). It has more positive than negative aspects:

- acquisition of 3D data across large areas;
- hundreds/thousands of measurements taken per second;
- non-contact operation type;
- high degree of resilience to external environmental factors;

Another example comes from direct borehole investigations allowing in situ observations and permafrost evolution monitoring thanks to the use of different instruments like cameras to obtain images, inclinometers or probes to get horizontal and vertical deformations (W. Haeberli C. G., 1993; L. Arenson, Borehole deformation measurements and internal structure of some rock glaciers in Switzerland, 2002; J. Noetzli L. A., 2021). However, this solution is quite difficult to be implemented and still very limited: drilling in these heterogeneous and sometime inaccessible environments is in fact both a technical both an economical challenge, but surely not impossible (L. Arenson, Borehole deformation measurements and internal structure of some rock glaciers in Switzerland, 2002).



Figure 97 : TLS from <https://geosurveyengineering.co.ke/terrestrial-laser-scanning/>

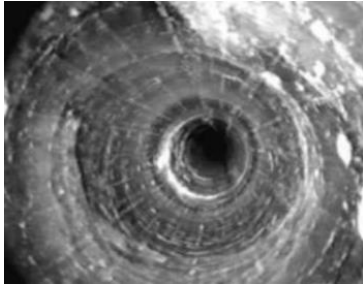


*Figure 98 : Photograph from a borehole camera from (L. Arenson, Borehole deformation measurements and internal structure of some rock glaciers in Switzerland, 2002) on the left; borehole implementation from (J. Noetzli L. A., 2021) on the right*

Together with this, also the installation of an early warning system directly connected to a control centre which would be alerted in case of a significant increase of velocity of some material. The aim is to communicate the situation to the local authorities on one side and, on the other, to give a specific sign (caution, warning or evacuate) to prevent and to avoid disasters related to the lava streams.

Moreover, what it is already in place but to be widely enhanced, is the development of containment walls (the so-called “dépotoirs”) to retain the material which drop towards the valley and then to move it in organised stockage in situ, so directly in the Val D’Anniviers (E. Bardou C. , 2011).



## Conclusions

This thesis has extensively examined the effects of climate change, particularly global warming, on the Bonnard rock glacier, in the Swiss Alps. Through a detailed analysis of 11 years of data obtained from aerial photogrammetry and GPS measurements, the study has identified significant mechanical and morphological deformations in the glacier, demonstrating a clear acceleration in the movement of surface materials such as rocks and boulders. This acceleration poses increasing risks, including lava streams and debris flows that threaten the nearby Zinal village.

Key findings of the research highlight the sensitivity of periglacial environments to climatic changes. The data indicates a direct relationship between rising atmospheric temperatures, decreasing snowfall and the destabilization and acceleration of rock glaciers. The warming has led to increased ice melt and reduced ice viscosity, exacerbating slope instability and triggering rock falls, landslides and debris flows.

The cessation of monitoring activities in 2018 presents a significant gap in understanding the recent behaviour of the glacier.

The adopted methodology integrates aerial photogrammetry, meteorological data analysis and GPS-based monitoring to evaluate the glacier's behaviour. Aerial photogrammetry provides qualitative insights through georeferenced images, allowing the identification of major surface displacements over time. Meteorological data analysis reveals trends in temperature, precipitation and snowpack height, establishing a correlation between these factors and the glacier's deformations. GPS monitoring offers quantitative data on surface movements, enabling precise calculations of displacement and velocity patterns.

From 2007 to 2018, the glacier's surface velocity has increased significantly, with the most considerable movements observed in specific lobes. This acceleration correlates with rising temperatures, suggesting that climate change is a primary driver of the observed changes. The study also identifies the areas most prone to instability, which are crucial for predicting and managing future risks.

The study underscores the importance of continuous monitoring, employing both geophysical and geomatic tools to assess these dynamic changes comprehensively: the restart of monitoring programs, including terrestrial laser scanning (TLS) and direct borehole investigations, is recommended to obtain high-resolution data and in situ observations. Additionally, the

implementation of early warning systems connected to control centers can provide timely alerts to local authorities and residents, mitigating the impact of potential disasters.

Containment walls, or "dépotoirs," are suggested as a means to retain material and manage debris flow more effectively. These structures can help control the movement of hazardous material towards the valley, providing a more organized approach to risk management.

In conclusion, this study sheds light on the profound effects of climate change on the Bonnard rock glacier and the surrounding environment. It underscores the necessity of ongoing monitoring and the development of robust adaptation strategies to protect vulnerable communities and ecosystems. The research contributes valuable knowledge to the field of environmental engineering, offering practical solutions for addressing the challenges posed by a rapidly changing climate.

## References

- (SSGm), S. s. (2020). *Géomorphologie de la montagne froide*. Retrieved from Géomorphologie périglaciaire: <https://geomorphologie-montagne.ch/4-1-une-forme-particuliere-le-glacier-rocheux/>
- A. Cicoira, M. M.-R. (2020). A general theory of rock glacier creep based on a in-situ and remote sensing observations, *Permafrost and Periglacial Processes*. *10.1002*, 2090.
- A. Kääb, T. R. (2005, May). Advance mechanisms of rock glaciers. (L. John Wiley & Sons, Ed.)
- A. Kääb, V. K. (2003). Rock glacier dynamics: implications from high-resolution measurements of surface velocity fields. *Permafrost. Proceedings of the 8th International Conference on Permafrost, 21-25 July 2003, Zurich, Switzerland* (pp. 501-506). Zurich: A.A. Balkema.
- ArcGIS Pro*. (n.d.). Retrieved from Curvature function: <https://pro.arcgis.com/en/pro-app/latest/help/analysis/raster-functions/curvature-function.htm#:~:text=The%20Planform%20curvature%20%28commonly%20called%20plan%20curvature%29%20is,the%20surface%20is%20laterally%20convex%20at%20that%20cell>
- B. Einhorn, C. P. (2011). Adaptation de la gestion des risques naturels face au changement climatique. *WP6 Risk Prevention and Risk Management*.
- E. Bardou, C. (2011). Adaptation de la gestion des risques naturels face au changement climatique. *WP6 "Risk Prevention and Risk Management"*, (pp. 10-15).
- E. Bardou, G. F.-B. (2015). Process oriented use of geostatistics to analyse creeping para-glacial features. *Earth surface processes and landforms*, *40*, 1191-1201.
- E. Bardou, G. F.-B.-D. (2011). Influence of the connectivity with permafrost on the debris-flow triggering in high-alpine environment. *5th International Conference on Debris-Flow Hazards Mitigation, Mechanics, Prediction and Assessment*.
- E. P. Howald, J. T. (2023). Frozen soil properties modification in the context of climate change. *8th International Symposium on Deformation of Geomaterials*.

- G. Bertoldi, V. D. (2012). An integrated method for debris flow hazard mapping using 2D runout models. *12th Congress INTERPRAEVENT*.
- I. Gärtner-Roer, N. B. (2022, May). Glacier-permafrost relations in a high-mountain environment: 5 decades of kinematic monitoring at the Gruben site, Swiss Alps.
- IPCC, I. P. (2023). *Sixth Assessment Report (AR6), Chapter 2 High Mountain Areas*.
- J. Noetzli, C. P. (2023). *Swiss Permafrost Bulletin 2022*. Technical report, Swiss Permafrost Monitoring Network PERMOS.
- J. Noetzli, L. A. (2021, May). Best practice for measuring permafrost temperature in boreholes based on the experience in the Swiss Alps. *Frontiers in Earth Science*.
- Kaufmann, V. (2012). The evolution of rock glacier monitoring using terrestrial photogrammetry: the example of Ausseres Hochebenkar rock glacier. *Austrian Journal of Earth Sciences*, 105/2(63-77).
- L. Arenson, M. H. (2002). Borehole deformation measurements and internal structure of some rock glaciers in Switzerland. *Permafrost and Periglacial processes*, 117-135.
- L. Arenson, M. H. (2002). Borehole deformation measurements and internal structure of some rock glaciers in Switzerland. *Permafrost and Periglacial processes*, 117-135.
- Le Temps*. (2017). Retrieved from <https://www.letemps.ch/suisse/valais/chantier-changements-climatiques>
- Le Temps*. (2017). Retrieved from Le chantier des changements climatiques: <https://www.letemps.ch/suisse/valais/chantier-changements-climatiques>
- M. Chiarle, G. M. (2008). Geomorphological impact of climate change on alpine and periglacial areas. Examples of processes and description of research needs.
- M. Davies, O. H. (2001, March). The effect of rise in mean annual temperature on the stability of rock slopes containing ice-filled discontinuities. *Permafrost and periglacial processes*.
- M. Rogora, G. T. (2020). Chemical characterization of rock glacier outflows. *WP3 - Assessment of the available water resources in the transboundary area*.
- M. Stoffel, M. B. (2009). Tree-ring reconstruction of past debris flows based on a small number of samples - possibilities and limitations. *Landslides*, 6(3), 225-230.

*MeteoSwiss*. (n.d.).

N. Shen, B. W. (2023). A review of terrestrial laser scanning (TLS)- based technologies for deformation monitoring in engineering. 223.

P. Deline, S. G. (2015). *Snow and ice related hazards, risks and disaster, Ice loss and slope stability in high-mountain regions*. Academic Press.

Parvex, M. (2013, April 17). *Le Temps*. Retrieved from <https://www.letemps.ch/suisse/sueurs-froides-zinal-permafrost-degele>

R. Delaloye, C. L.-R. (2010). Overview of rock glacier kinematics research in the Swiss Alps: seasonal rhythm, interannual variations and trends over several decades. (G. Helvetica, Ed.) 135-145.

R. Delaloye, S. M. (2013). Rapidly moving of rock glaciers in Mattertal. (pp. 21-31). Eidg. .

R. Delaloye, S. M. (2013). Rapidly moving rock glaciers in Mattertal. (pp. 21-31). Eidg. Forschungsanstalt für Wald, Schnee und Landschaft WSL.

R. Delaloye, T. S. (2010). The contribution of InSAR data to the early detection of potentially hazardous active rock glaciers in mountain areas.

R. Kenner, M. P. (2017). Factors controlling velocity variation at short-term, seasonal and multiyear time scales, Ritigraben rock glacier, western Swiss Alps. *Permafrost and Periglacial Processes*, 675-684. doi:10.1002/ppp. 1953

R. Lugon, M. S. (2010). Rock glacier dynamics and magnitude frequency relations of debris flows in a high-elevation watershed: Ritigraben, Swiss Alps. *Global and Planetary Change*, 73(3-4), 202-210.

R.S. Anderson, L. A. (2018, May). Glaciation of alpine valleys: the glacier - debris covered glacier - rock glacier continuum.

UNEP, U. N. (2008). *UNEP 2007 annual report*.

W. Haeberli, B. H. (2006). Permafrost creep and rock glacier dynamics. *Permafrost and Periglacial processes*, (pp. 189-214). doi:10.1002/ppp. 561

W. Haeberli, C. G. (1993). Mountain Permafrost and Climatic Change. *Permafrost And Periglacial Processes*, 4, 165-174.

X. Bodin, E. T. (2009). Two Decades of Responses (1986–2006) to Climate by the Laurichard.  
*Permafrost and Periglacial Processes*, 331-344.